CC BY

ORIGINAL PAPER

International Journal of Occupational Medicine and Environmental Health 2026;39(5):461–492
https://doi.org/10.13075/ijomeh.1896.02841

QUANTITATIVE EFFECTS OF SLEEP DEPRIVATION ON DIGITAL PUPILLARY DYNAMICS AND VISUAL EVOKED POTENTIAL METRICS IN HEALTHY ADULTS

KRZYSZTOF RÓŻANOWSKI and MICHAŁ JANKOWSKI

Ministry of the Interior and Administration, Warsaw, Poland
Regional Center for Digital Medicine, National Medical Institute

Highlights
- Forty-eight-hour sleep loss selectively altered the pupillary light reflex (PLR) dilation-phase dynamics.
- Dilation-phase parameters D_{Dil1}, D_{Dil2} and redilation velocities emerged as novel fatigue markers.
- Prolonged N145 visual evoked potential latency indicated cortical visual slowing.
- Relative pupillary unrest index and PLR changes converged with subjective sleepiness.
- Autonomic shifts preceded measurable cognitive decline.

Abstract
Objectives: The pupillary light reflex (PLR), pupillary sleepiness test (PST), and visual evoked potentials (VEPs) are crucial for assessing the functional integrity of the visual and autonomic nervous systems. These responses integrate retinal phototransduction with midbrain reflex pathways and cortical visual processing, all of which are influenced by physiological and clinical disorders. Their temporal dynamics lay the groundwork for using pupillary reflexes and cortical potentials as biomarkers of fatigue and the effects of psychoactive substances on them. This study aimed to identify physiological biomarkers of fatigue by evaluating the PLR and VEPs. **Material and Methods:** These modalities were validated against the PST, pupillary unrest index parameters, and blink-rate analysis to assess autonomic and cortical contributions to fatigue. This study examined the effects of 48-hour sleep deprivation on pupillary behavior in 18 healthy adults under controlled conditions. **Results:** Analysis of PLR dynamics revealed that the dilation-phase parameters D_{Dil1} and D_{Dil2}, corresponding to pupil diameters at 20% and 80% recovery, respectively, were sensitive to changes in autonomic activation. These complemented the established fatigue indices, including constriction velocity, relative amplitude, time of minimum diameter, and latency. Visual evoked potentials analysis demonstrated that sustained wakefulness modulated cortical responses, with a delay and amplitude reduction in the N145 component. **Conclusions:** Biomarkers from the pupillary reflex dilation phase and N145 LAT in VEP recordings serve as reliable indicators of fatigue severity, as corroborated by the PST and *Stanford Sleepiness Scale* assessments. Int J Occup Med Environ Health. 2026;39(5):461–92

Key words:
fatigue, sleepiness, occupational safety, cognitive performance, visual evoked potentials, pupillary dynamics

Conflict of interest: the authors declare no potential conflicts of interest related to the research, authorship, or publication of this article.
Received: February 27, 2026. Accepted: September 22, 2026.
Corresponding author: Michał Jankowski, Ministry of the Interior and Administration, Regional Center for Digital Medicine, National Medical Institute, Wołoska 137, 02-507 Warsaw, Poland (e-mail: jankowski.michal@me.com).

INTRODUCTION

Modern societies demand sustained daytime functioning, whereas nighttime enables physiological restoration. Fatigue, marked by drowsiness or exhaustion, often results from insufficient sleep [1]. Sleep deprivation impairs cognitive functions, including attention, alertness, intelligence, reasoning, and reaction time [2]. Brain imaging shows that sleep loss induces neurophysiological changes [3]. Sleep deprivation categories include long-term total deprivation (>45 h), short-term (≤45 h), and partial (<7 h daily) [4]. Five hours of sleep every night for a week impairs cognitive performance [5]. Shift work impairs decision-making and reduces physical and mental activities [6]. Sleep deprivation affects psychomotor and cognitive performances. It slows reactions, increases threat-response latency (LAT), reduces alertness, impairs hazard identification, disrupts information processing, and diminishes short-term memory [7]. Performance decline during sleep deprivation compared to alcohol effects. Driving after 24 h without sleep deteriorates more than driving with a breath alcohol concentration exceeding 22 μg/100 ml, equivalent to 50 mg alcohol/100 ml blood [8]. Sleep restriction worsens mood, whereas total deprivation reduces energy, concentration, and cognitive processing [3]. It increases negative affect, fatigue, drowsiness, and confusion [9].

Sleepiness is evaluated using both objective and subjective methods. Objective methods include the multiple sleep latency test and maintenance of wakefulness test. Subjective assessments included the *Stanford Sleepiness Scale* (SSS), *Karolinska Sleepiness Scale*, *Epworth Sleepiness Scale*, visual analog scale, and *Sleep-Wake Activity Inventory*. These methods effectively quantify sleepiness but are limited to laboratory settings only. Estimating fatigue requires trained personnel and equipment, making it impractical for the continuous monitoring of drivers, pilots, and operators. While the pupillary light reflex (PLR) has been studied in conditions such as Parkinson's disease, Alzheimer's disease, and multiple sclerosis, few studies have examined the effects of sleep deprivation on PLR [10]. Under controlled conditions, the PLR tests revealed sensitivity to fatigue. Currently, handheld devices provide basic pupillary response information, but smartphone-based solutions may replace standard pupillometry. Mobile technology enables the development of portable diagnostic systems for assessing PLR during fatigue. Visual evoked potentials (VEPs) reflect visual pathway integrity and detect neural changes due to sleep deprivation. The aim of this study was to identify sleepiness biomarkers using PLR and VEP parameters and to compare them with pupillary sleepiness test (PST) results. This hypothesis suggests that additional parameters exist for describing pupillary reflex curves, which are modulated by autonomic nervous system activity during sleep deprivation.

MATERIAL AND METHODS

Procedures were performed under controlled clinical conditions using certified electromyography (EMG) and VEP diagnostic systems. Measurements were conducted by qualified medical and technical personnel under controlled laboratory conditions, following the institutional safety and ethical standards. Standardized psychometric and electrophysiological tools were used for continuous physiological monitoring. During the 48-hour sleep-deprivation protocol, participants remained under continuous staff supervision. Food and fluids were provided, and participants were allowed scheduled breaks without sleep. Between measurement sessions, participants remained in a monitored room and were allowed only low-arousal activities, including reading, watching films, computer use, and board games. Recumbent rest, naps, and sleep were not permitted. Participant well-being was monitored throughout the protocol, and the study team could discontinue participation in the event of clinically relevant discomfort, excessive distress, or safety concerns.

Ethics, consent, and participant safety

The study protocol was reviewed and approved by the Ethics Committee for Human Research at the Military Institute of Aviation Medicine in Warsaw, Poland (decision No. 11/2015, June 17, 2015). The ethics committee issued a positive opinion on conducting the study in accordance with the submitted documentation, which included the study application, project description, study assumptions, research methodology, characteristics of the study group, participant statement, and participant information sheet. All procedures were conducted in accordance with the Declaration of Helsinki. Before enrolment, participants received written and verbal information about the study aims, procedures, expected duration, sleep-deprivation protocol, and possible discomfort related to prolonged wakefulness. Participation was voluntary, and written informed consent was obtained before any study procedure. Participants were informed that they could withdraw from the study at any time without providing a reason and without negative consequences. Participants did not receive financial compensation. No participant withdrew from the study.

Selection and description of participants

The study included 18 healthy adults (9 women and 9 men), aged 20–32 years (mean [M] ± standard deviation [SD] 27.55±3.29). Participants were recruited on a voluntary basis from university students and research staff through institutional announcements and direct information distributed within the collaborating academic and research environment. Recruitment was based on willingness to participate in a demanding 48-hour supervised sleep-deprivation protocol and on fulfilment of predefined medical, sleep-related, ophthalmological, and safety criteria. All candidates underwent screening before inclusion. The screening procedure included a structured medical and sleep-related interview, review of current medication and substance use, verification of sleep diaries from the week preceding the laboratory phase, and ophthalmological assessment. Inclusion criteria were:

- adult age,
- self-reported good general health,
- regular sleep-wake rhythm,
- habitual nocturnal sleep of approx. 7–8 h,
- absence of diagnosed sleep, neurological, or psychiatric disorders,
- normal or corrected-to-normal vision within the accepted corrective range.

Exclusion criteria were defined to minimize factors that could confound pupillary, autonomic, cognitive, or visual electrophysiological measurements. Participants were excluded in the presence of:

- ocular disease or pupillary abnormality potentially affecting PLR or VEP recordings;
- history of epilepsy, seizure disorder, or other neurological disease;
- chronic systemic disease;
- night-shift work;
- transmeridian travel within the preceding 3 months;
- current use of medications or substances known to affect sleepiness, pupil size, autonomic tone, or visual electrophysiology;
- current dependence on nicotine, alcohol, or psychoactive substances;
- inability to comply with pre-study caffeine, alcohol, nicotine, and stimulant abstinence requirements.

No formal a *priori* sample-size calculation was performed. The final sample size was constrained by the logistical and safety requirements of a resource-intensive, 48-hour, continuously supervised sleep-deprivation protocol with repeated multimodal physiological measurements. The within-subject repeated-measures design increased statistical efficiency by allowing each participant to serve as his or her own control. To address sample-size interpretation, a sensitivity power analysis was added and is reported in Table 1.

Table 1. Sensitivity power analysis for paired baseline-to-deprivation contrasts by available sample size in a study of sleepiness biomarkers, Warsaw, Poland, 2015

Sample size	α	Target power	Test	Minimum detectable d_z
16 participants	0.05	0.80	paired t-test/within-subject contrast	0.75
17 participants	0.05	0.80	paired t-test/within-subject contrast	0.72
18 participants	0.05	0.80	paired t-test/within-subject contrast	0.70

Cohen's d_z was calculated for paired within-subject contrasts as mean change divided by standard deviation of the change score.

Data collection and measurements

The study was conducted in 9 experimental rounds with 2 participants each. Each round had 2 stages. In the first stage, participants arrived at 8:00 a.m. Monday–Wednesday for 3-hour examinations. After 1.5 h, participants took the Visual Pursuit Test (*Linienverfolgungstest* – LVT) thrice, followed by the Determination Test (DT) for reaction times. Participants then completed the *NASA Task Load Index* (NASA-TLX). The second stage was the sleep-deprivation phase. The supervised laboratory phase lasted approx. 39 h and was embedded within a 48-hour continuous wakefulness protocol. Total sleep-deprivation exposure was calculated from the standardized morning wake time before admission to the final assessment, whereas the 39-hour period refers to the continuously supervised in-laboratory phase. Participants stayed awake under supervision, with measurements taken at 3-hour intervals. Between the sessions, the participants performed low-intensity activities in a monitored area. The measurements included VEP, PLR, and pupillary unrest index (PUI). The PLR and PST/PUI measurements were obtained repeatedly across the sleep-deprivation protocol, whereas VEP recordings were obtained at predefined assessment points according to the electrophysiological schedule. Cognitive performance and workload were evaluated after 24 h and 48 h of being awake. The first participant measurement began at 8:00 p.m. and the second at 9:00 p.m. During breaks, the participants stayed in a break room using laptops, watching movies, reading, and playing games. Each participant performed the LVT 3 times during the first measurement. After the final morning LVT, the participants took the DT. Visual evoked potentials, PLR, and PUI were measured at 3-hour intervals. Participants conducted a city trip to maintain interest and manage sleepiness using transportation with unlimited rest. Daily measurements began at 2:00 p.m. and night sessions began at 8:00 p.m. Standardized tools were used to evaluate cognitive functioning, workload, and neurophysiological responses.

Between-session wakefulness control

Between measurement sessions, participants remained in a monitored room under staff supervision. They were allowed to engage only in low-arousal, low-physical-demand activities, including reading, watching films, using a computer, quiet conversation, and playing board or card games. Recumbent rest, naps, and sleep were not permitted. Participants were instructed to remain seated or standing and were observed by the study staff to ensure wakefulness. Caffeine, alcohol, nicotine, energy drinks, and stimulant substances were prohibited throughout the deprivation protocol. Food and non-stimulant fluids were provided. During the daytime period, a supervised low-intensity walk was scheduled to support wake maintenance while minimizing physical exertion and cognitive load.

Psychological, pupillometric, electrophysiological, and physiological assessment tools

During progressive wakefulness, a standardized multimodal assessment battery characterized subjective sleep-

iness (SSS), subjective workload (NASA-TLX), psychophysiological performance (Vienna Test System: DT and LVT [Schuhfried GmbH, Mödling, Austria]; pupillary dynamics (PLR and PST), cortical visual response timing (pattern-VEP), and resting cardiovascular status (blood pressure [BP] and heart rate [HR]). The PST-derived relative pupillary unrest index (rPUI) was treated as the principal tonic marker of pupillary instability, whereas resting cardiovascular measures were included as supportive physiological controls rather than as primary biomarkers. Each instrument, together with its acquisition parameters and analysis, is described in the following subsections.

Psychological and cognitive performance tests

Cognitive and psychomotor performance were assessed using computerized psychological tests in the Vienna Test System to quantify fatigue correlates and validate the findings from pupillography and VEP. The battery comprises tests sensitive to the effects of sleep deprivation on vigilance, attention, reaction speed, and workload. Each test captured a distinct dimension: the DT measured reaction speed and cognitive control, the LVT evaluated sustained attention and visual processing, and the NASA-TLX measured the cognitive workload. These tools evaluate cognitive, perceptual, and affective fatigue, with the DT and LVT yielding metrics of reaction control and attention, while the NASA-TLX and SSS provide insight into mental workload and sleepiness. This structure allowed for a correlation with PLR dilation metrics, rPUI, and VEP characteristics. The test parameters are listed in Table 2. The DT assesses reaction speed under alternating visual and auditory stimuli. In the S1 form, participants were required to respond to light and sound signals using specific response keys. The DT performance was recorded at baseline and after 24 h and 48 h of wakefulness. The LVT examines visual processing speed and visuomotor coordination. The S2 form of the LVT required participants to trace target paths among distractor lines during the baseline and deprivation phases. The NASA-TLX assesses workload through 6 subscales: mental demand, physical demand, temporal demand, performance, effort, and frustration. Participants performed comparisons to determine dominance and rated the categories on a 20-point scale, yielding a workload index. The NASA-TLX results were analyzed using physiological measures to characterize fatigue. The SSS, a 7-point instrument for alertness self-evaluation, was completed at each measurement point to validate the changes in pupillary dynamics and VEP parameters against sleepiness perception.

Visual evoked potentials measuring device

Visual evoked potentials reflect the electrical activity of the visual cortex in response to visual stimulation. Triggered by light flashes activating the retina and reaching the occipital cortex, VEP testing is non-invasive and assesses visual system integrity. In fatigue research, VEPs provide an objective neurophysiological marker of cortical responsiveness [11]. Their inclusion complemented cognitive and autonomic indices to capture prolonged wakefulness impact. The VEP analysis identified neurophysiological fatigue biomarkers from sleep deprivation, reflecting signal transmission from retina to primary visual cortex (Brodmann area 17). The VEP components are generated by axons that transmit retinal signals to cortical neurons [12]. The key parameters, negative peak at approx. 75 ms (N75), positive peak at approx. 100 ms (P100), and negative peak at approx. 145 ms (N145) latencies, and N75–P100 peak-to-peak amplitude (75–100), are summarized in Table 2.

The VEPs are influenced by both physiological and technical factors [13]. Eye movements reduce the signal amplitude, whereas mental activity can alter the waveform morphology. Technical factors include screen luminance, contrast, check size, electrode placement, and stimulus frequencies. The P100 LAT increases as stimulus brightness decreases, whereas the amplitude diminishes with re-

Table 2. Cognitive and psychomotor performance measures obtained during 48 h of sustained wakefulness in a study of sleepiness biomarkers, Warsaw, Poland, 2015

Parameter	Description
Vienna Test System	
Determination Test	the S1 version was used (all types of stimuli, time-limited form): reactions (total) correct reactions, wrong reactions, missed stimuli, number of stimuli, test duration (min), median response time (s)
Visual Pursuit Test	the S2 form was used, contains 40 test items: test duration (s), number of correct answers, median time of correct answers (s), median time of incorrect answers (s), execution time (s), number of tasks
NASA Task Load Index	2 parts, based on 6 subscales (mental load, physical load, time pressure, efficiency, effort, frustration)
Stanford Sleepiness Scale	a 7-point scale; quick and easy way to assess how alert you are feeling
Visual evoked potential	
N75	time after which the negative waveform reflecting the activity in the fovea and primary visual cortex appears (ms)
P100	time to occurrence of positive P100 peak which is generated by the pyramidal cells in layer IV of primary visual cortex; early phase of the P100 peak appears to be in dorsal extrastriate cortex of the middle occipital gyrus, whereas the late phase of P100 generated by the ventral extrastriate cortex of the fusiform gyrus (ms)
N145	time to occurrence of the negative peak reflecting activity in the visual association cortex (Brodmann areas 18 and 19) (ms)
75–100	amplitude between value of N75 peak and P100 peak value (peak to peak) (μV)
Pupillary light reflex	
stimulus duration	duration of light impulse, standard 200 ms
latency	time from stimulus onset (begin of measurement) till the reaction onset, typically 200–300 ms (±2 ms)
contraction velocity	pupillary constriction velocity, typically 3 mm/s (3%)
reaction duration	latency till minimum diameter, typically 500 ms (±3 ms)
redilation velocity	
1 – fast (V_{Dil1})	velocity at the beginning of the redilation 20–35% initial pupil value, typically: 1–1.5 mm/s (3%)
2 – slow (V_{Dil2})	velocity at the end of the redilation period 80–95% initial pupil value, typically: ≤0.5 mm/s (3%)
contraction time	time from latency till two-third of the reaction amplitude is reached, typically 250 ms (±2 ms)
redilation time	time from the minimum diameter till one-third of the amplitude is reached, typically 400–500 ms (±2 ms)
amplitude	difference between initial diameter and the minimum diameter, typically: 0.8–1.5 mm (±0.05 mm)
initial pupil diameter	diameter at the beginning of the measurement, typically 4–9 mm (±0.05 mm)
relative amplitude	percentage relation of the amplitude to the initial diameter, typically 15–25%
time of minimum diameter	refers to the length of time during which the diameter is <50% of the initial value
dilatation diameter	
1 – fast (D_{Dil1})	pupil diameter at the moment when it reaches 20% of its initial value in the dilation phase (mm)
2 – slow (D_{Dil2})	pupil diameter at the moment when it reaches 80% of its initial value in the dilation phase (mm)
Pupillary sleepiness test	
blinks	number of times when the pupil was covered by the eyelid within 60 s
pupillary unrest index	fatigue index determined based on the amplitude of the oscillation of changes in the pupil diameter (mm/s)
hippus wave interpolation	the percentage of time when the pupil remained obscured by the eyelid

Table 2. Cognitive and psychomotor performance measures obtained during 48 h of sustained wakefulness in a study of sleepiness biomarkers, Warsaw, Poland, 2015 – cont.

Parameter	Description
Zephyr BioHarness 3 and oscillometric blood monitoring	
HR (mean and peak)	the average and highest recorded number of heartbeats per min; HR was recorded continuously using the Zephyr BioHarness 3 and at each time point during the night (bpm)
average HR variability (SDNN)	standard deviation of the time intervals between consecutive normal heartbeats (NN intervals) (ms)
respiratory rate	the rate at which breathing occurs, set and controlled by the respiratory center of the brain (breaths per min)
blood pressure (systolic and diastolic)	the force of the blood pushing against the artery walls during contraction and relaxation of the heart; measurements were taken at each time point during the night (mm Hg)
physiological load	parameter estimated using Zephyr BioHarness 3 – a measure of the effort accumulated during a session (the sum over time of physiological intensity), which is an instantaneous measure of effort, as indicated by HR level (cardiovascular workout level – scale 0–10)
mechanical load	parameter estimated using Zephyr BioHarness 3 – a measure of effort accumulated (the sum over time of mechanical intensity), which is an instantaneous measure of effort, as indicated by peak acceleration levels (a measure of musculoskeletal workout level – scale 0–10)

HR – heart rate; NN – normal-to-normal; SDNN – standard deviation of normal-to-normal intervals.
Zephyr BioHarness 3 – wearable biosensor for physiological load measurement (Zephyr Technology Corporation, Annapolis, USA).

duced retinal illumination [11]. Measurements were performed under standardized conditions. Components N75, P100, and N145 reflect the early activation of the primary visual cortex, synchronous depolarization of pyramidal neurons, and delayed inhibitory activity in the associative visual areas. The VEPs were recorded using a Nicolet Viasys Viking Select EMG system (Natus Medical Incorporated, Middleton, WI, USA). Recordings used gold-plated electrodes at left occipital (O1), right occipital (O2), midline occipital (Oz), and midline frontal (Fz) positions with an impedance <5 kΩ. All procedures followed the International Society for Clinical Electrophysiology of Vision (ISCEV) standards.

During recording, participants sat 1 m from a monitor, fixating on a central red point on a reversing checkerboard pattern (16 × 12 matrix of black and white squares, each measuring 2 × 2 cm). Testing was performed in a dark room with the non-tested eye covered. The left eye was stimulated and the right eye occluded. The participants maintained fixation as the pattern alternated across the full field, and then the left and right halves. Each sequence was repeated twice, with an average of 150 repetitions. The reversal frequency was 1.9 Hz, check size was 1°, mean luminance was 50 cd/m², and contrast was 80%. The procedure was repeated for the right eye. Averaging improves the signal-to-noise ratio. Recordings were performed at baseline and after 48 h of wakefulness, with each session lasting 15–20 min. The VEP recordings, along with psychometric and autonomic measures, characterized neural fatigue dynamics.

Pattern-VEP recordings were obtained separately for the left and right eye. Monocular recordings were used to verify the functional symmetry of the afferent visual pathways and to exclude clinically relevant interocular asymmetry that could confound sleep-deprivation effects. Interocular differences were treated as a quality and physiological control rather than as a primary endpoint. In the absence of systematic interocular asymmetry, the main VEP interpretation focused on time-dependent changes across the sleep-deprivation protocol.

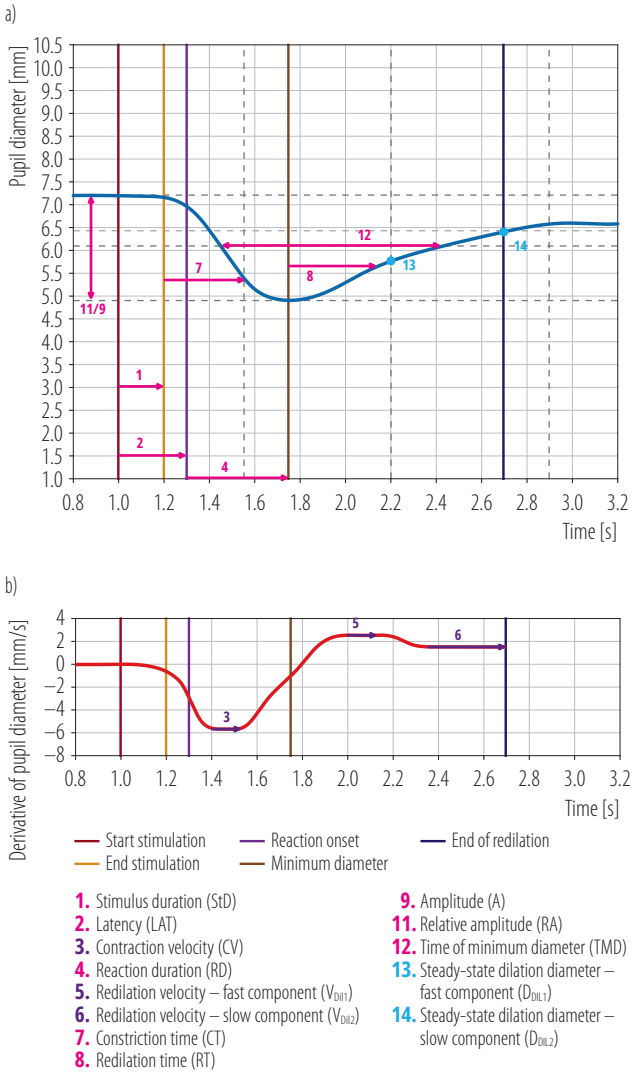


Figure 1. Components and quantitative parameters of the pupillary light reflex, illustrated using simulated curves: a) pupil diameter as a function of time, showing constriction and subsequent redilation following a single light stimulus; b) first derivative of pupil diameter with respect to time, showing negative values during constriction and positive values during redilation, Warsaw, Poland, 2015

Dynamic pupillography (PLR and PST)

The PLR reflects visual and autonomic nervous system function and relies on the pupillary sphincter muscle, retinal photoreceptors, and visual pathway components [14]. Light exposure causes retinal rods and cones to hyperpolarize, sending signals through the bipolar and ganglion cells. Intrinsically photosensitive retinal ganglion cells (ipRGCs) with melanopsin integrate these signals to regulate the PLR. The PLR adjusts the pupil size to light, dilating in low light and constricting in bright light for optimal retinal illumination. Parasympathetic pathways via the Edinger-Westphal nucleus and oculomotor nerve cause constriction, whereas sympathetic activation inhibits the parasympathetic tone, stimulating the dilator pupillae muscle for dilation [15]. This study assessed the PLR to quantify fatigue-induced changes in autonomic pupil regulation, differentiate between central and peripheral pupillary response components, and provide an alertness biomarker. The PLR curve and analyzed parameters are shown in Figure 1, with the quantitative descriptors listed in Table 2.

The PST assesses physiological sleepiness and fatigue. It analyzes spontaneous pupil oscillations, alternating constriction and dilation, known as the hippus fatigue wave. The rPUI quantifies pupil diameter fluctuations as an indicator of vigilance. Lowenstein described hippus as cyclic pupillary oscillations in constant light. Although recognized for decades, its mechanisms remain poorly understood. The oscillatory pattern reflects autonomic balance: parasympathetic inhibition reduces oscillation amplitude, while sympathetic activation has minimal effect. Research has shown that hippus wave amplitude increases with fatigue and decreases with cortical arousal [16]. Enhanced amplitude and frequency of pupillary oscillations occur in fatigue, sleep deprivation, and central nervous system disorders, including preictal epilepsy [17]. A positive association between frontal lobe dysfunction and pupillary oscillation amplitude has been previously reported [18,19].

The PLR and PUI measurements were performed using an F²D Fit-for-Duty Pupillograph (AmTech, Dossenheim, Germany). The system is a portable infrared pupillography platform used to evaluate central nervous system activation. The device consists of a head-mounted infrared sensor operating at 25 Hz with a spatial resolution of 0.05 mm.

The PST lasted 11 min, and the PLR measurement was conducted for each eye with 5 light-flash sequences at 60-second intervals. Examinations were performed in a darkened room after dark adaptation was performed. The procedure followed international technical standards. The PLR and PST data provided measures of autonomic and cortical contributions to fatigue, characterizing physiological sleepiness during sustained wakefulness. The parameters from the PST analysis are summarized in Table 2.

Physiological monitoring

Continuous physiological monitoring was used to assess autonomic reactivity and systemic fatigue during prolonged wakefulness. Participants used the Zephyr BioHarness 3 system (Zephyr Technology Corporation, Annapolis, USA), a wearable biosensor for physiological load measurement. The device combines electrocardiographic, respiratory, and motion sensors, enabling the real-time acquisition of cardiovascular, respiratory, posture, and activity parameters. The Zephyr BioHarness 3 recorded the HR, respiratory rate, body posture, activity level, and 3-axis acceleration, tracking autonomic nervous system modulation. It uses a dry-electrode ECG sensor and triaxial accelerometer to detect body movement and orientation. Blood pressure was measured using an Omron M4 automatic oscillometric sphygmomanometer (Omron Healthcare, Kyoto, Japan) to calibrate the cardiovascular parameters. All physiological data were synchronized with the cognitive and electrophysiological measurements. The BioHarness software analyzed the data using proprietary algorithms, computing the physiological and mechanical load indices based on HR and acceleration signals. These parameters indicate the participants' cardiovascular and musculoskeletal workload during the sleep deprivation protocol. The monitored physiological signals and derived parameters are summarized in Table 2.

Data analysis

The study was designed as an exploratory repeated-measures biomarker study with predefined primary physiological domains rather than as a single-endpoint confirmatory trial. These domains were selected on physiological grounds and included pupillary light-reflex timing and dilation-phase recovery parameters, PST-derived pupillary unrest, and selected pattern-VEP latencies. All statistical tests were 2-sided. Primary-domain results were interpreted as hypothesis-guided biomarker findings, whereas secondary and supportive outcomes were interpreted as exploratory.

For outcomes measured across repeated sessions, 1-way repeated-measures analysis of variance (ANOVA) was used with measurement cycle as the within-subject factor, partitioning total variability into between-sessions (mean square for inter-sessions – MSINT) and within-subject (mean square intra-subject – MSINS) components and yielding the F-ratio (MSINT/MSINS). Measurement cycle was defined by consecutive experimental sessions representing increasing sleep-deprivation exposure (sessions 1–9). For PLR and PST measures, participant-level values were analyzed to avoid treating repeated technical recordings from the same participant as independent observations. For VEP outcomes, repeated-measures models were restricted to the predefined VEP assessment points.

Model assumptions were assessed before inference. Distributional assumptions were evaluated using the Shapiro-Wilk test, and homogeneity of variance was assessed using Levene's test where applicable. When the assumption of sphericity was violated, Greenhouse-Geisser correction was applied. Baseline-to-deprivation comparisons were performed using Dunnett's *post hoc* test.

To address multiple testing in the exploratory framework, false discovery rate (FDR) correction was applied using the Benjamini-Hochberg procedure within predefined outcome families. The FDR correction was applied separately to omnibus repeated-measures ANOVA results, key base-

Table 3. Characteristics of the participants in a study of sleepiness biomarkers, Warsaw, Poland, 2015

Variable	Participants (N = 18) [n (%)]	M±SD/M
Sociodemographic		
age [years]		27.6 ± 3.2
sex (female)	9 (50)	
weight [kg]		76.8 ± 16.8
height [cm]		173.8 ± 8.3
profession status		
employed	9 (50)	
student	4 (22.2)	
unemployed	5 (27.8)	
Medical		
vision defect [D]		R –0.75 ± 1.5, L –1.0 ± 1.5
no defect	3 (16.7)	
myopia	10 (55.5)	R –2.0 ± 1.25, L –2.0 ± 1.25
hyperopia	5 (27.8)	R +1.0 ± 0.75, L +0.5 ± 0.25
Sleep patterns		
wake up time		7:10 a.m. ± 1 h 24 min
bed getting out		7:35 a.m. ± 1 h 29 min
going to bed		10:30 p.m. ± 1 h 31 min
estimated time of falling asleep		11:10 p.m.
sleep time		7 h 8 min ± 1 h 29 min

R – right eye; L – left eye.

line-to-deprivation contrasts, exploratory convergent-validity correlations, and sex-stratified exploratory comparisons. Results with FDR-adjusted $q < 0.05$ were considered significant within the corresponding outcome family.

For key baseline-to-deprivation contrasts, paired-samples Cohen's d_z was calculated as the mean within-subject change divided by the standard deviation of the change scores. A sensitivity power analysis was performed to estimate the minimum detectable within-subject effect size given the available sample size, $\alpha = 0.05$, and 80% power. Convergent validity was explored using correlations between baseline-normalized changes in pupillometric, VEP, subjective sleepiness, DT, and LVT outcomes. Pearson correlations were used for approximately normally distributed change scores; otherwise, Spearman correlations were used. Sex-stratified analyses were descriptive and exploratory, comparing baseline-normalized endpoint changes between women and men, because the study was not powered for formal sex-difference inference.

Calculations were performed using Statistica software. Descriptive statistics are expressed as M±SD. Statistical significance was set at $p < 0.05$ for nominal tests and $q < 0.05$ for FDR-adjusted exploratory family-wise interpretation. Primary analyses focused on changes in PLR timing and dilation-phase recovery parameters, PST-derived pupillary unrest indices (rPUI, INT, and BLK), and pattern-VEP LAT components (N75, P100, and N145).

RESULTS

Participant characteristics and baseline sleep

The cohort was homogeneous in terms of age, sex, and occupation. The mean age was 27.6 years (range: 26–32 years), body weight 76.8 kg (range: 50–110 kg), and height 173.8 cm (range: 155–188 cm). Women comprised 50% of participants. Three were students, while the others were university graduates in professional employment (Table 3). Ophthalmological assessment revealed normal vision in 3 participants, hyperopia in 27% (R +1.0 D, L +0.5 D), and myopia in 50% (R –2.0 D, L –2.0 D). No ophthalmological abnormalities that could affect the results were observed. Lifestyle data showed healthy patterns: 63% were non-smokers, 33% abstained from coffee, 55% avoided energy drinks, and 11% reported no alcohol use, while others consumed alcohol 2–4 times a month. Participants had no history of chronic medication use, illness, or recent transmeridian travel. Sleep diary records confirmed regular sleep-wake rhythms, with a mean nocturnal sleep duration of 7 h 8 min and a bedtime of approx. 12:00 a.m. At least 1 daytime nap during the obser-

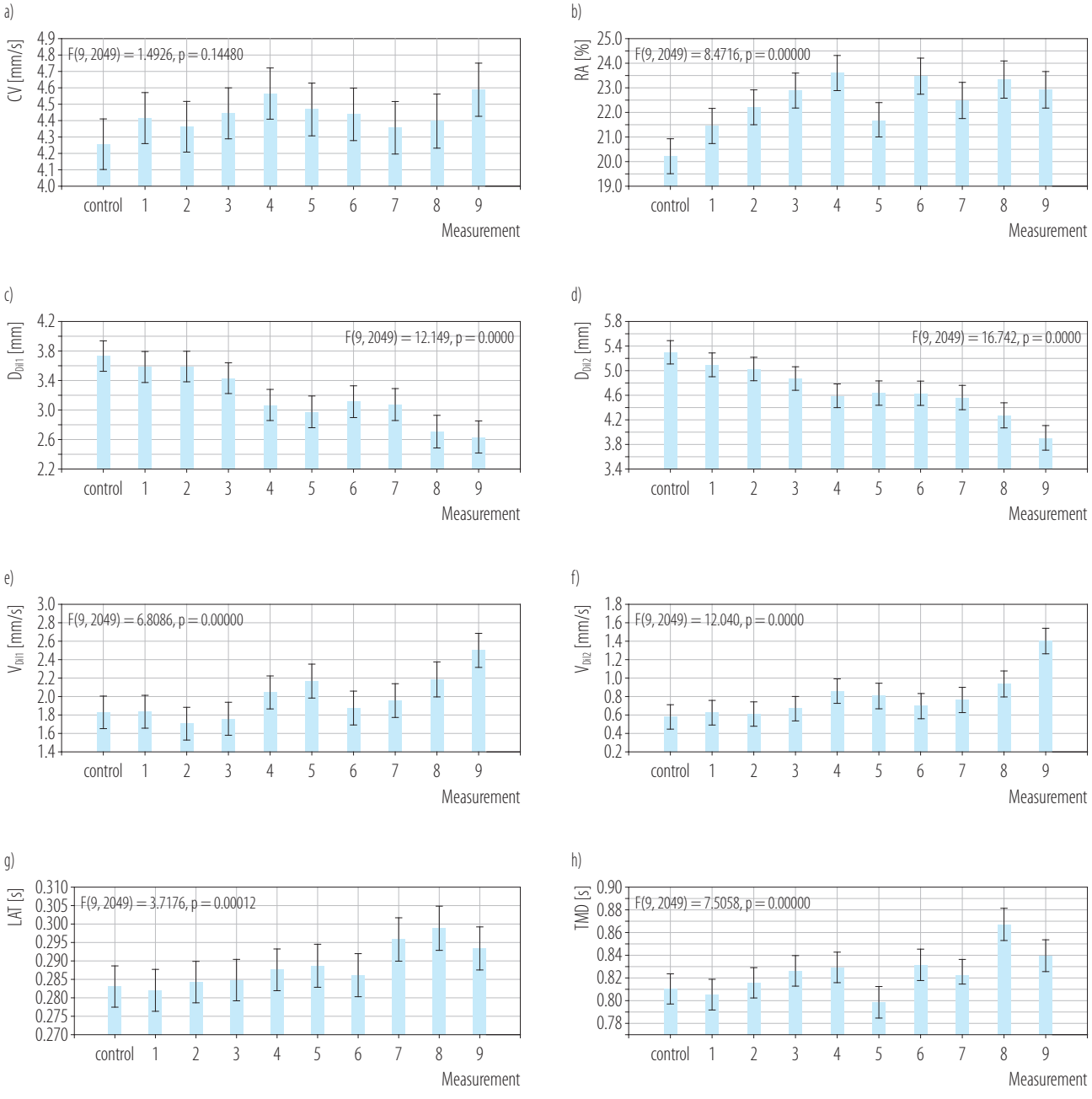
vation period was reported by 44%, as shown in Table 3. The participants entered the experimental phase with stable physiology and regular circadian alignment.

Pupillary light reflex

Analysis of the PLR revealed significant time-dependent changes during sleep deprivation. After participant-level analysis and FDR correction, the most robust PLR effects involved LAT, time of minimum diameter (TMD), and dilation-phase recovery parameters, particularly pupil diameter during the fast dilation phase (D_{Dil1}), pupil diameter during the slow dilation phase (D_{Dil2}), redilation velocity during the fast phase (V_{Dil1}), and redilation velocity during the slow phase (V_{Dil2}). Constriction velocity did not reach significance in the participant-level omnibus analysis, and reaction duration showed only limited point-wise evidence; therefore, both were interpreted as supportive rather than primary stable markers. Significant differences were observed in the relative amplitude (RA), redilation velocities (V_{Dil1}, V_{Dil2}), dilation diameters (D_{Dil1}, D_{Dil2}), TMD, and LAT (Table 2). The temporal evolutions of these parameters are shown in Figure 2. *Post hoc* testing (Dunnett's test) confirmed these effects compared to the control measurement (Table 4). The first significant deviation appeared at measurement 2 (day 1, 12:30 a.m.) in the RA group, which increased from 20.23% (SD = 5.31%) at baseline to 22.22% (SD = 5.09%) at measurement 2, corresponding to a 9.8% change in pupil constriction ($p < 0.05$). Relative amplitude remained elevated throughout the study, suggesting sustained parasympathetic modulation alteration. For the redilation parameters, V_{Dil2} and V_{Dil1} increased significantly, peaking at 3:00 a.m. (measurement 8) and 6:00 a.m. (measurement 9), respectively. The V_{Dil2} reached significance with a 0.28 mm/s increase at measurement 4 (+20%), whereas V_{Dil1} increased by 0.36 mm/s at measurement 8 (+14%). These changes indicate autonomic dysregulation resulting from prolonged wakefulness. The D_{Dil1} and D_{Dil2} showed a progressive decline, with maximum differences of 1.1 mm and 1.39 mm, respectively. Significant decreases were observed from measurement 4 (−0.67 mm for D_{Dil1} and −0.43 mm for D_{Dil2}). Time of minimum diameter varied by 70 ms, with significant prolongation on the second day at measurements 8 (M±SD 0.87±0.15 s) and 9 (M±SD 0.84±0.16 s). Latency increased with prolonged wakefulness, reaching significance during measurements 7 and 8. These findings demonstrate the sensitivity of the PLR to sleep deprivation, with measurable impairments supporting pupillographic indices as reliable markers of central nervous system fatigue.

Visual evoked potentials

The VEP parameters were analyzed to assess the cortical responsiveness during sleep deprivation. Four indices were evaluated: N75, P100, N145, and 75–100 amplitude, defined as the potential difference between the N75 and P100 peaks. Recordings were obtained from 3 bipolar leads: O1–Fz, O2–Fz, and Oz–Fz, representing the left, right, and midline occipital regions (Figure 3). The numerical outcomes are summarized in Table 5, with representative waveforms for Oz–Fz shown in Figure 4. The N145 component exhibited the most pronounced sensitivity to sleep deprivation: N145 LAT progressively delayed over sessions, whereas the N75 LAT and 75–100 amplitude remained stable. For the left eye under full-field checkerboard mode, the N145 peak shifted from 157.17 ms at baseline to 164 ms after 24 h ($\Delta = 6.83$ ms) and 168 ms after 48 h ($\Delta = 10.83$ ms), although the differences were not statistically significant. Latency changes were more pronounced in the right eye. The N145 peak shifted from 152.17 ms at baseline to 166.35 ms after 24 h ($\Delta = 14.18$ ms) and to 171.44 ms after 48 h ($\Delta = 19.27$ ms), with differences reaching statistical significance ($p < 0.05$). Similar results were obtained with right-half checkerboard stimulation. Significant N145 LAT prolongation persisted in left-eye recordings under a split-field configuration after 48 h of wakefulness. The earliest component,



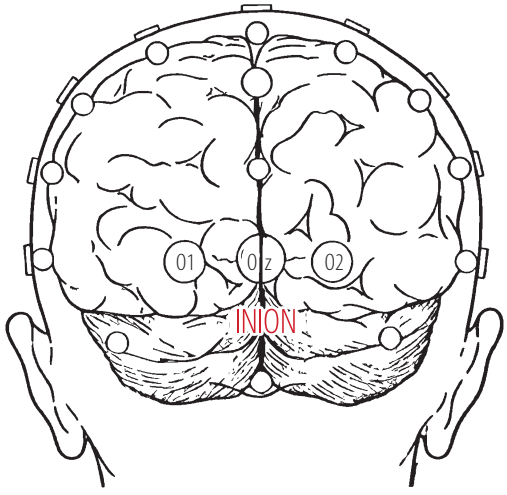
Relative amplitude showed the earliest significant deviation, with increased constriction depth beginning at measurement 2 and remaining elevated throughout the protocol. Redilation velocity V_{Dil1} increased progressively reaching its largest deviation at measurement 8. Redilation velocity V_{Dil2} exhibited significant elevation beginning at measurement 4 and peaking at measurement 8. Steady-state dilation diameter D_{Dil1} showed a progressive decline with significant reductions beginning at measurement 4. Steady-state dilation diameter D_{Dil2} decreased gradually across sessions with marked reductions during the second day of wakefulness. Time of minimum diameter demonstrated significant prolongation at measurements 8 and 9. Latency of the pupillary response increased significantly during late-night and early-morning sessions.

Figure 2. Temporal dynamics of pupillary light reflex parameters during 48 h of sustained wakefulness: a) contraction velocity (CV), b) relative amplitude (RA), c) steady-state dilation diameter – fast component (D_{Dil1}), d) steady-state dilation diameter – slow component (D_{Dil2}), e) redilation velocity – fast component (V_{Dil1}), f) redilation velocity – slow component (V_{Dil2}), g) latency (LAT) of the pupillary response, and h) time of minimum diameter (TMD), in the study on sleepiness biomarkers among 18 healthy adults (9 women, 9 men), Warsaw, Poland, 2015

Table 4. *Post hoc* statistical comparisons (Dunnett's test) for pupillary light reflex (PLR) parameters across measurement sessions in the study on sleepiness biomarkers among 18 healthy adults (9 women, 9 men), Warsaw, Poland, 2015

Measurement	Pupillary light reflex													
	relative amplitude [%]		redilation velocity [mm/s]				diameter [mm]				time of min. diameter [s]		latency [s]	
			Dil1		Dil2		Dil1		Dil2					
	M±SD	p	M±SD	p	M±SD	p	M±SD	p	M±SD	p	M±SD	p	M±SD	p
Baseline (free day)	20.23±5.31	–	1.83±1.15	–	0.58±0.25	–	3.74±1.53	–	5.30±1.11	–	0.81±0.07	–	0.28±0.03	–
Sleep deprivation														
first night														
1 (10:00 p.m.)	21.46±4.83	0.11	1.83±1.19	1.00	0.62±0.36	0.99	3.59±1.35	0.92	5.10±1.02	0.59	0.81±0.06	0.99	0.28±0.03	0.99
2 (12:30 a.m.)	22.22±5.09	**<0.05**[a]	1.71±0.92	0.93	0.61±0.38	0.99	3.59±1.33	0.93	5.03±1.19	0.26	0.82±0.07	0.99	0.28±0.03	0.99
3 (3:00 a.m.)	22.90 ±5.26	**<0.05**[a]	1.76±0.95	0.99	0.67±0.52	0.94	3.44±1.31	0.26	4.87±1.13	**<0.05**[a]	0.83±0.07	0.47	0.28±0.03	0.99
4 (6:00 a.m.)	23.61 ±5.06	**<0.05**[a]	2.05±1.33	0.44	0.86±1.10	**<0.05**[a]	3.07±1.72	**<0.05**[a]	4.59±1.48	**<0.05**[a]	0.83±0.10	0.27	0.28±0.04	0.85
day														
5 (3:00 p.m.)	21.66 ±5.53	**<0.05**[a]	2.17±1.72	0.06	0.81±1.45	0.13	2.98±1.82	**<0.05**[a]	4.64±1.58	**<0.05**[a]	0.80±0.12	0.80	0.28±0.06	0.67
second night														
6 (10:00 p.m.)	23.48 ±4.29	**<0.05**[a]	1.88±1.07	0.99	0.70±0.40	0.80	3.12±1.33	**<0.05**[a]	4.64±1.11	**<0.05**[a]	0.83±0.10	0.19	0.28±0.03	0.98
7 (12:30 a.m.)	22.50 ±5.86	**<0.05**[a]	1.96±1.09	0.92	0.76±0.75	0.31	3.08±1.47	**<0.05**[a]	4.57±1.44	**<0.05**[a]	0.82±0.07	0.78	0.30±0.05	**<0.05**[a]
8 (3:00 a.m.)	23.35 ±5.68	**<0.05**[a]	2.19±1.37	**<0.05**[a]	0.94 ±1.01	**<0.05**[a]	2.71±1.65	**<0.05**[a]	4.27±1.72	**<0.05**[a]	0.87±0.15	**<0.05**[a]	0.30±0.05	**<0.05**[a]
9 (6:00 a.m.)	22.93 ±6.05	**<0.05**[a]	2.50±2.13	**<0.05**[a]	1.41±2.12	**<0.05**[a]	2.64±1.95	**<0.05**[a]	3.91±2.20	**<0.05**[a]	0.84±0.16	**<0.05**[a]	0.29±0.03	0.08

"–" indicates not applicable (baseline reference measurement).
Dil1 – fast dilation phase; Dil2 – slow dilation phase.
Bolded are statistically significant p-values ($p < 0.05$).
[a] One-way ANOVA.



Fz – midline frontal position; 01 – left occipital position; 02 – right occipital position; 0z – midline occipital position.
Inion – the most prominent point of the external occipital protuberance.

Figure 3. Bipolar occipital electrode montage (01–Fz, 02–Fz, 0z–Fz) used for visual evoked potential recordings in the study on sleepiness biomarkers among 18 healthy adults (9 women, 9 men), Warsaw, Poland, 2015

N75, and the 75–100 amplitude showed minimal changes with high inter-individual variability. The N75 LAT for the left eye under full-field condition differed by only 0.22 ms (M = 72 ms) across sessions. These parameters did not show any significant differences from the baseline. Pattern-VEP analysis showed significant time-dependent prolongation of P100 and N145 latencies after FDR correction, whereas N75 and 75–100 amplitude were not significant. The N145 showed the clearest effect, with LAT prolongation evident during prolonged wakefulness; P100 was also significantly delayed. These findings indicate that prolonged wakefulness affected later stages of cortical visual response timing more clearly than the earliest VEP component. Exploratory left-right eye comparisons of full-field pattern-VEP recordings did not show systematic interocular asymmetry for N75, P100, N145, or 75–100 amplitude (all $p > 0.24$). Therefore, the interpretation of VEP findings focused on time-dependent changes associated with prolonged wakefulness rather than on eye laterality.

Pupillary sleepiness test and subjective sleepiness

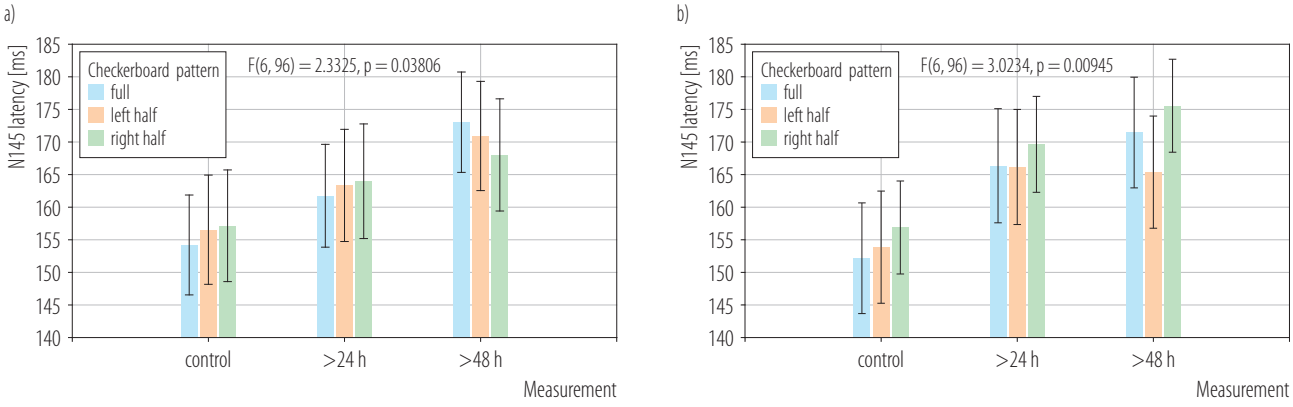
The outcomes of the PST and SSS questionnaires are shown in Table 6 and Figure 5. Pupillographic indices were analyzed using VEP and PLR parameters to assess the sleepiness. The rPUI showed sensitivity to sleep deprivation, increasing significantly by measurement 4 (6:00 a.m.) to 1.31 mm/s from a baseline of 0.79 mm/s (SD = 0.46 mm/s) ($p < 0.05$). Significant elevations during measurements 5, 7, 8, and 9 confirmed the prolonged wakefulness effects on pupil instability. The hippus wave interpolation (INT) parameter showed a parallel trend corresponding to the percentage of eyelid closure (PERCLOS) index. This metric quantifies the obscuration of the pupil by the eyelid. The INT value increased significantly ($p < 0.05$) in measurements 5, 7, 8, and 9. When the eyelid covered the pupil for 20% of the recording period, elevated rPUI suggested an association with sleep pressure. Blink frequency (BLK) increased from 13 blinks/min at baseline to 22 blinks/min under sleep deprivation, with a notable increase during measurement 7 (M±SD 21.64±9.62 blinks/min). The mean pupil diameter decreased throughout the study, reducing by 0.4 mm from 6.93 mm (SD = 0.78 mm) at baseline to 6.53 mm (SD = 0.14 mm) during measurement 8.

The $rPUI_{all}$ was the principal PST-derived marker of tonic pupillary instability during sustained wakefulness. Mean pupil diameter, hippus wave interpolation, and blink-related indices also changed across the protocol, but these measures were treated as supportive indices of tonic pupil state, blink/eyelid behavior, and signal-quality burden rather than as the primary sleepiness marker. The SSS scores ranged 2–5 pts, with post-test ratings averaging 0.59 pts higher than the pre-test scores. Subjective sleepiness increased across the deprivation period, with perceived fatigue rising by 150% prior to PST and 141% after PST. The parallel increase in PST-derived indices and subjective sleepiness supports the interpretation of dynamic pupillography as a candidate marker of progressive sleepiness, although cross-modal associations should be interpreted as exploratory.

Table 5. Results of the *post hoc* test for comparison with the control group in 18 healthy adults (9 women, 9 men), Warsaw, Poland, 2015

Measurement	Visual evoked potential [ms]																							
	N75						P100						N145						75–100					
	full chessboard		left half		right half		full chessboard		left half		right half		full chessboard		left half		right half		full chessboard		left half		right half	
	M±SD	p	M±SD	p	M±SD	p	M±SD	p	M±SD	p	M±SD	p	M±SD	p	M±SD	p	M±SD	p	M±SD	p	M±SD	p	M±SD	p
Sleep deprivation																								
left eye																								
baseline (free day)	73.22 ±6.58	–	74.58 ±10.84	–	73.53 ±6.33	–	107.46 ±4.93	–	113.00 ±13.78	–	108.77 ±7.26	–	157.17 ±17.92	–	156.56 ±15.79	–	154.22 ±15.15	–	7.56 ±4.14	–	3.79 ±2.40	–	4.44 ±1.97	–
>24 h	71.71 ±2.32	0.69	75.79 ±10.71	0.92	74.38 ±7.96	0.93	110.91 ±5.22	0.34	116.09 ±7.71	0.76	110.91 ±7.18	0.67	164.00 ±17.50	0.43	163.35 ±17.60	0.42	161.76 ±14.14	0.29	7.01 ±3.25	0.86	3.42 ±1.77	0.83	4.23 ±2.05	0.93
>48 h	73.44 ±2.19	0.99	73.08 ±9.56	0.87	74.92 ±8.71	0.81	112.57 ±8.42	0.09	119.07 ±13.38	0.34	110.71 ±6.99	0.71	168.06 ±18.55	0.13	170.94 ±19.14	**<0.05**[a]	173.06 ±18.57	**<0.05**[a]	7.01 ±3.14	0.86	3.41 ±2.18	0.82	3.47 ±1.83	0.24
right eye																								
baseline (free day)	71.19 ±5.82	–	72.78 ±5.80	–	73.67 ±8.63	–	109.21 ±5.86	–	107.64 ±3.30	–	113.14 ±7.28	–	152.17 ±15.50	–	153.89 ±14.97	–	156.89 ±11.18	–	7.90 ±3.70	–	4.61 ±2.10	–	3.99 ±2.19	–
>24 h	75.03 ±8.51	0.32	74.24 ±9.09	0.80	79.68 ±7.70	0.16	114.00 ±10.81	0.27	111.79 ±7.12	0.15	113.07 ±9.46	0.99	166.35 ±17.14	**<0.05**[a]	166.18 ±17.74	0.09	169.65 ±17.51	**<0.05**[a]	5.99 ±2.59	0.16	3.95 ±1.61	0.56	3.38 ±1.36	0.54
>48 h	74.36 ±10.64	0.44	75.33 ±7.75	0.51	79.33 ±13.34	0.18	112.71 ±9.07	0.48	111.36 ±7.31	0.21	114.43 ±10.35	0.90	171.44 ±20.62	**<0.05**[a]	165.39 ±20.92	0.11	175.56 ±15.86	**<0.05**[a]	7.58 ±3.32	0.94	5.09 ±2.48	0.72	3.60 ±2.01	0.76

For description of the N75, P100, N145, and 75–100 parameters see Table 2.
Bolded are statistically significant p-values ($p < 0.05$).
[a] One-way ANOVA.



For description of Fz, Oz, N75, N145, and P100 see Table 2 and Figure 3.
Visual evoked potential waveform for the left eye (Oz–Fz channel) under full-field checkerboard stimulation, showed stable N75 and P100 components across sessions.

Figure 4. Representative visual evoked potential (VEP) waveforms during progressive sleep deprivation: a) for the left eye (Oz–Fz channel) under full-field checkerboard stimulation, and b) for the right eye (Oz–Fz channel), in the study on sleepiness biomarkers among 18 healthy adults (9 women, 9 men), Warsaw, Poland, 2015

Psychometric performance and subjective workload

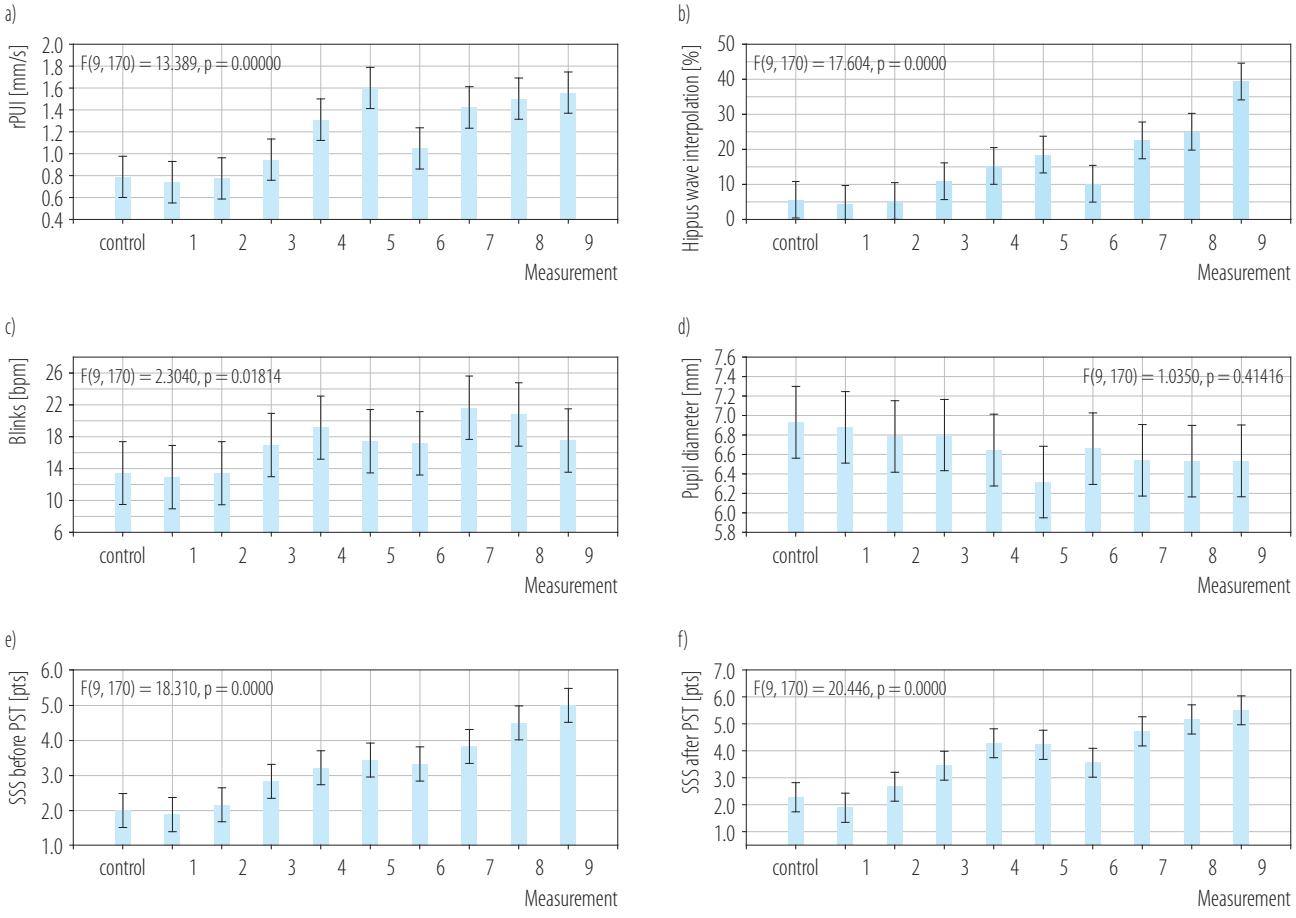
To evaluate cognitive efficiency and subjective task load under progressive sleep deprivation, 3 psychometric instruments were administered: the NASA-TLX, DT, and LVT. The NASA-TLX measures subjective mental workload across 6 domains: mental, physical, and temporal demand, effort, performance, and frustration, rated on a 20-point bipolar-interval scale. Analysis showed that NASA-TLX subscales after LVT increased significantly during the second day of wakefulness, except for efficiency and time pressure (Figure 6a,b, Table 7). Mental load increased by +140%, physical load by +190%, effort by +85%, and frustration by +185% ($p < 0.05$ for measurements 8–9), indicating substantial cognitive strain. Efficiency decreased by 21% during measurement 1 (M±SD 5.89±4.09) relative to the control (7.50±5.73) and recovered later (10.83±6.12). Time pressure remained stable, averaging M±SD 7.30±0.77 across sessions. The NASA-TLX results after DT showed higher perceived workload, with physical load increasing from M±SD 9.56±5.42 to 13.33±6.04 after 48 h of wakefulness (39.4% increase, $p < 0.05$). Changes between the control and final sessions were as follows: mental load +32.2%, effort +20.0%, frustration +32.9%, efficiency +18.9%, and time pressure −1.6%. The DT evaluates the complex reaction speed under alternating stimuli by measuring the total, correct, and erroneous reactions, missed stimuli, and response time (Figure 7a–c).

The analysis showed no significant differences, although performance declined during the final testing. The LVT measures visual processing under time pressure and evaluates task duration, responses, and execution time (Figure 7d–f). Response LAT increased toward the deprivation end, with the median correct response time increasing by 280 ms. The total completion time increased from 129.0 s to 145.7 s (+13%). Brief psychophysiological tasks showed non-monotonic and task-dependent changes. The DT and LVT outcomes did not show a deterioration pattern comparable to the pupillometric and VEP markers, suggesting that short structured tasks may be influenced by practice effects or transient compensatory effort. Overall, extended wakefulness elevated subjective mental workload, whereas objective psychomotor performance changed less systematically.

Table 6. Results of the *post hoc* test for comparison with the control group for variables derived from the pupillary sleepiness test (PST) and the *Stanford Sleepiness Scale* (SSS) in 18 healthy adults (9 women, 9 men), Warsaw, Poland, 2015

Measurement	PST								SSS [pts]			
	rPUI [mm/s]		hippus wave interpolation [%]		blinks [blinks/min]		pupil diameter [mm]		before PST		after PST	
	M±SD	p	M±SD	p	M±SD	p	M±SD	p	M±SD	p	M±SD	p
Baseline (free day)	0.79±0.46	–	5.63±7.47	–	13.42±10.16	–	6.93±0.78	–	2.00 ±0.77	–	2.28±0.89	–
Sleep deprivation												
first night												
1 (10:00 p.m.)	0.74±0.40	0.99	4.45±3.38	0.99	12.93±8.71	1.00	6.88±0.67	0.99	1.89±0.83	0.99	1.89±0.90	0.90
2 (12:30 a.m.)	0.78±0.33	1.00	5.28±4.53	1.00	13.41±7.24	1.00	6.78±0.77	0.99	2.17±0.99	0.99	2.67±1.14	0.90
3 (3:00 a.m.)	0.95±0.29	0.80	10.91±13.04	0.63	16.95±8.39	0.76	6.80±0.77	0.99	2.83±0.99	0.10	3.44±1.20	**<0.05**[a]
4 (6:00 a.m.)	1.31±0.40	**<0.05**[a]	15.27±11.57	0.06	19.14±7.97	0.25	6.65±0.18	0.86	3.22±0.94	**<0.05**[a]	4.28±1.28	**<0.05**[a]
day												
5 (3:00 p.m.)	1.60±0.57	**<0.05**[a]	18.53±11.95	**<0.05**[a]	17.43±5.60	0.64	6.32±1.07	0.12	3.44±1.04	**<0.05**[a]	4.22±1.06	**<0.05**[a]
second night												
6 (10:00 p.m.)	1.05±0.40	0.28	10.19±7.32	0.77	17.18±9.21	0.70	6.66±0.81	0.89	3.33±1.24	**<0.05**[a]	3.56±1.25	**<0.05**[a]
7 (12:30 a.m.)	1.42±0.32	**<0.05**[a]	22.56±13.72	**<0.05**[a]	21.64±9.62	**<0.05**[a]	6.54±0.18	0.58	3.83±1.20	**<0.05**[a]	4.72±1.23	**<0.05**[a]
8 (3:00 a.m.)	1.50±0.33	**<0.05**[a]	25.04±10.88	**<0.05**[a]	20.80±8.38	0.07	6.53±0.18	0.55	4.50±1.10	**<0.05**[a]	5.17±1.04	**<0.05**[a]
9 (6:00 a.m.)	1.56±0.44	**<0.05**[a]	39.36±18.61	**<0.05**[a]	17.52±8.84	0.61	6.53±0.14	0.57	5.00±1.14	**<0.05**[a]	5.50±1.50	**<0.05**[a]

rPUI – relative pupillary unrest index.
Bolded are statistically significant p-values ($p < 0.05$).
[a] One-way ANOVA.

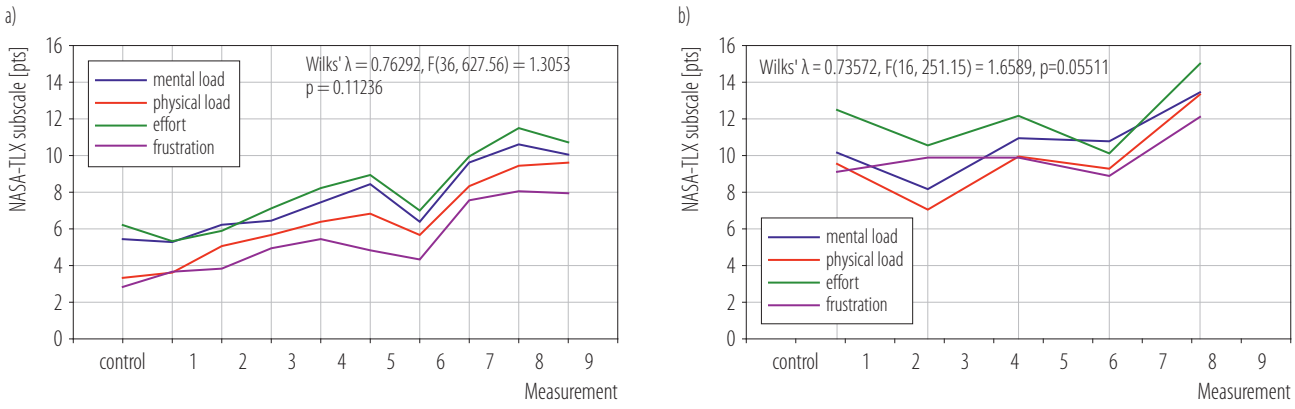


Relative pupillary unrest index demonstrated significant increases beginning at measurement 4 and remaining elevated throughout prolonged wakefulness. Hippus wave interpolation reflected eyelid-induced obscuration of the pupil area, with significant elevations during measurements 5, 7, 8, and 9. Blink frequency showed a progressive rise with marked increases during late-night sessions. Mean pupil diameter across sessions displayed a gradual decline with the smallest diameter observed during measurements 8 and 9. *Stanford Sleepiness Scale* scores before the PST showed progressive subjective sleepiness, and scores after the PST demonstrated additional increases in perceived fatigue following each measurement session.

Figure 5. Pupillary sleepiness test (PST) and *Stanford Sleepiness Scale* (SSS) outcomes during 48 h of sustained wakefulness: a) relative pupillary unrest index (rPUI), b) hippus wave interpolation (INT), c) blink frequency, d) pupil diameter across sessions, e) SSS scores before the PST, f) SSS scores after the PST, in the study on sleepiness biomarkers among 18 healthy adults (9 women, 9 men), Warsaw, Poland, 2015

Physiological monitoring

During the experiment, physiological monitoring was performed using the Zephyr BioHarness 3 system and oscillometric BP measurements. Monitored parameters included HR (mean and peak HR), HR variability (standard deviation of normal-to-normal intervals – SDNN), respiration rate (RR), physiological load, and mechanical load (Figure 8). Analysis of variance showed significant effects on SDNN, reflecting HR variability. The F-test yielded $p < 0.05$ between the control and subsequent measurements, with variability increasing after midnight on the second day (measurements 7, 8, and 9). The increases in SDNN were 27.6%, 28.0%, and 14.0%, indicating enhanced parasympathetic modulation during advanced fatigue. The HR showed daytime elevations during measurement 5 due to physical activity, followed by a nocturnal decline. The RR decreased during the night. As sleep deprivation progressed, decreased physiological load and in-



The *NASA-TLX* scores obtained after each LVT session across 48 h of sustained wakefulness showed significant increases in mental load, physical load, effort, and frustration during the second day of wakefulness (measurements 8–9), indicating elevated cognitive strain.
The *NASA-TLX* subscale scores obtained after each DT session showed increasing workload across sessions, with physical load showing the largest rise from baseline to 48 h.
All values represent mean scores on a 20-point bipolar scale. Statistical significance based on repeated-measures multivariate analysis of variance (MANOVA).

Figure 6. The *NASA Task Load Index* (NASA-TLX) workload ratings across progressive sleep deprivation: a) subscale scores obtained after each Visual Pursuit Test (*Linienverfolgungstest* – LVT) session, and b) scale scores obtained after each Determination Test (DT) session, in the study on sleepiness biomarkers among 18 healthy adults (9 women, 9 men), Warsaw, Poland, 2015

creased mechanical load suggested the redistribution of autonomic resources. The core body temperature declined by 0.24°C (measurement 3) and 0.23°C (measurement 7). Blood pressure showed subtle fluctuations, with a maximum reduction in systolic pressure of 7% (measurement 6) and diastolic pressure of 7% (measurement 5) relative to baseline values of 125 mm Hg (systolic) and 84 mm Hg (diastolic) (Figure 9). Physiological data corroborated psychophysiological and electrophysiological findings, showing that while prolonged wakefulness induced autonomic shifts, homeostatic regulation was maintained. Selective modulation of HR variability and load indices demonstrated the interplay between central fatigue mechanisms and physiological adaptation during sleep deprivation.

Additional exploratory statistical analyses

After Benjamini-Hochberg FDR correction within outcome families, the principal PLR effects remained significant for LAT, TMD, D_{Dil1}, D_{Dil2}, V_{Dil1}, and V_{Dil2} (Tables 8 and 9). Contraction velocity (CV) did not reach significance in the participant-level omnibus analysis and was therefore interpreted as a supportive rather than a primary stable marker. Among PST-derived indices, rPUI remained strongly significant after FDR correction. For pattern-VEP recordings, P100 and N145 LAT prolongation remained significant after correction, whereas N75 and the 75–100 amplitude did not. The Visual Pursuit Test outcomes did not remain significant after FDR correction. Exploratory convergent-validity analysis showed the strongest uncorrected association between increasing rPUI and decreasing D_{Dil1}; however, this association did not remain significant after FDR correction across the full correlation family (Table 10). Sex-stratified descriptive and exploratory endpoint-change analyses are presented in Table 11. The main direction of change in pupillometric and VEP biomarkers was observed in both women and men. No endpoint-change comparison showed a sex-dependent effect that remained significant after FDR correction.

DISCUSSION

This study aimed to identify physiological and neurovisual fatigue biomarkers from prolonged sleep deprivation

Table 7. The *NASA Task Load Index* (NASA-TLX) results after Visual Pursuit Test (*Linienverfolgungstest* – LVT) and the Determination Test (DT) in 18 healthy adults (9 women, 9 men), Warsaw, Poland, 2015

Measurement	NASA-TLX subscale [pts]											
	mental load		physical load		time pressure		efficiency		effort		frustration	
	M±SD	p	M±SD	p	M±SD	p	M±SD	p	M±SD	p	M±SD	p
After LVT												
baseline (free day)	5.54±4.59	–	3.33±2.81	–	10.22±5.56	–	7.50±5.73	–	6.22±4.97	–	2.83±1.92	–
sleep deprivation												
first night												
1 (10:00 p.m.)	5.28±3.95	0.99	3.61±2.70	0.99	7.83±5.01	0.68	5.89±4.09	0.94	5.33±3.88	0.99	3.67±3.43	0.99
2 (12:30 a.m.)	6.22±4.68	0.99	5.06±3.84	0.87	6.50±5.32	0.21	6.72±4.79	0.99	5.89±4.51	0.99	3.83±3.55	0.99
3 (3:00 a.m.)	6.44±4.73	0.99	5.67±4.45	0.60	6.78±5.42	0.28	7.67±4.89	0.99	7.11±4.89	0.99	4.94±3.47	0.68
4 (6:00 a.m.)	7.44±4.96	0.81	6.39±5.01	0.30	7.22±5.79	0.43	8.83±4.96	0.98	8.22±5.20	0.83	5.44±4.87	0.45
day												
5 (3:00 p.m.)	8.44±4.96	0.39	6.83±4.79	0.17	7.39±5.76	0.50	8.89±5.20	0.97	8.94±5.46	0.53	4.83±4.37	0.74
second night												
6 (10:00 p.m.)	6.39±4.54	0.99	5.67±4.87	0.60	7.00±5.13	0.35	7.94±5.15	0.99	7.00±5.46	0.99	4.33±3.91	0.92
7 (12:30 a.m.)	9.61±5.61	0.10	8.33±5.46	**<0.05**[a]	8.06±4.60	0.78	9.67±5.50	0.76	9.94±5.93	0.20	7.56±6.16	**<0.05**[a]
8 (3:00 a.m.)	10.61±6.04	**<0.05**[a]	9.44±6.11	**<0.05**[a]	7.72±4.65	0.64	10.44±5.22	0.43	11.50±5.99	**<0.05**[a]	8.06±6.10	**<0.05**[a]
9 (6:00 a.m.)	10.06±6.53	**<0.05**[a]	9.61±6.45	**<0.05**[a]	7.17±5.64	0.41	10.83±6.12	0.29	10.72±5.94	0.07	7.94±1.60	**<0.05**[a]
After DT												
baseline (free day)	10.17±5.57	–	9.56±4.05	–	14.17±5.90	–	12.33±5.16	–	12.50±4.82	–	9.11±5.62	–
sleep deprivation												
first night												
1 (10:00 p.m.)	8.17±4.51	0.58	7.06±4.01	0.29	12.28±4.94	0.64	11.11±4.98	0.84	10.56±5.39	0.57	9.89±5.62	0.99
4 (6:00 a.m.)	10.94±4.78	0.97	9.94±4.45	0.99	13.39±4.98	0.98	12.44±3.87	0.99	12.17±4.77	0.99	9.89±6.15	0.98
second night												
6 (10:00 p.m.)	10.78±4.66	0.98	9.28±4.25	0.99	11.89±5.09	0.52	11.50±4.31	0.95	10.11±4.99	0.39	8.89±5.04	0.99
9 (6:00 a.m.)	13.44±5.80	0.17	13.33±5.65	**<0.05**[a]	13.94±5.90	0.99	14.67±4.70	0.37	15.00±4.28	0.35	12.11±6.98	0.36

Bolded are statistically significant p-values ($p < 0.05$).
[a] One-way ANOVA.

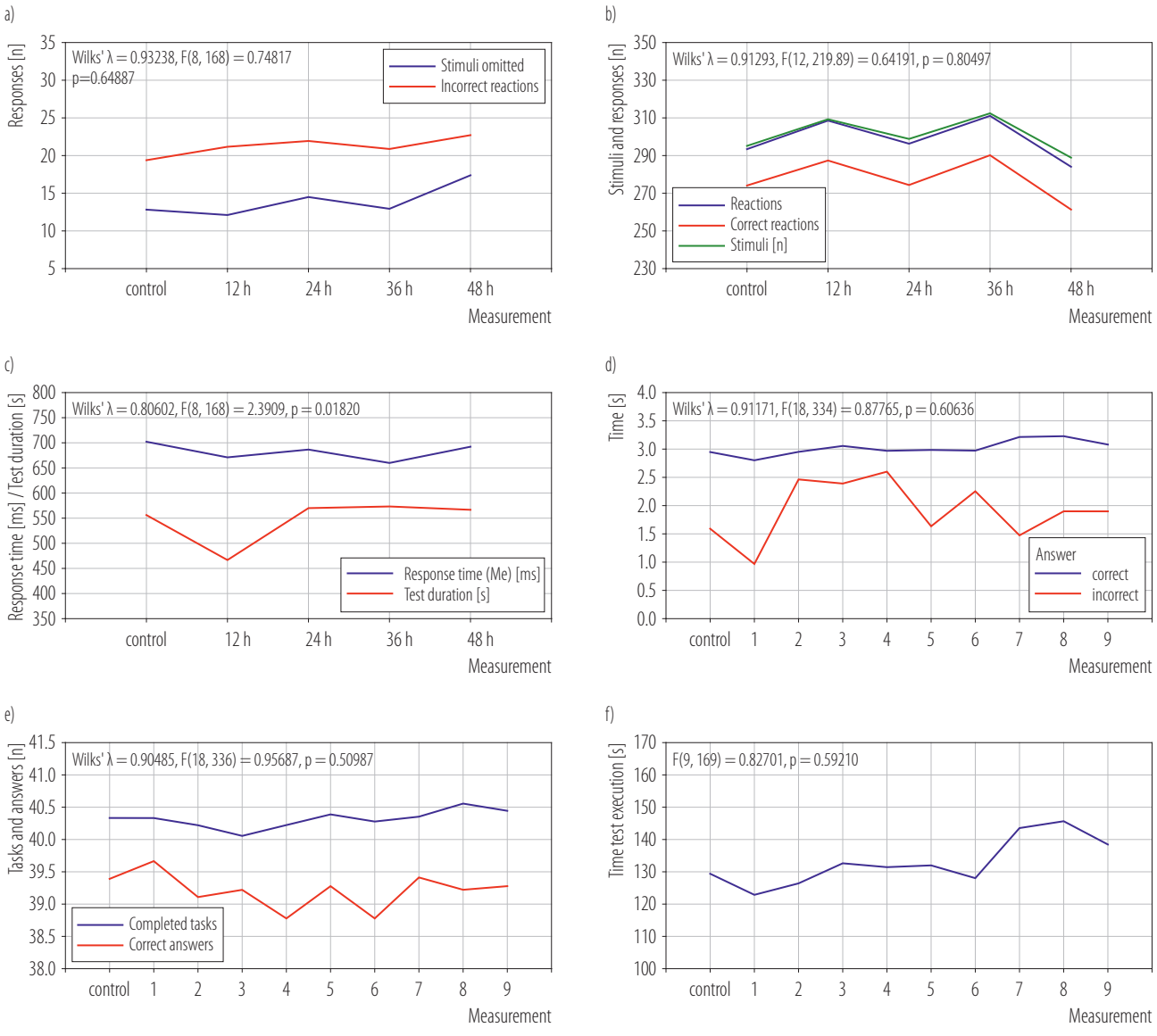
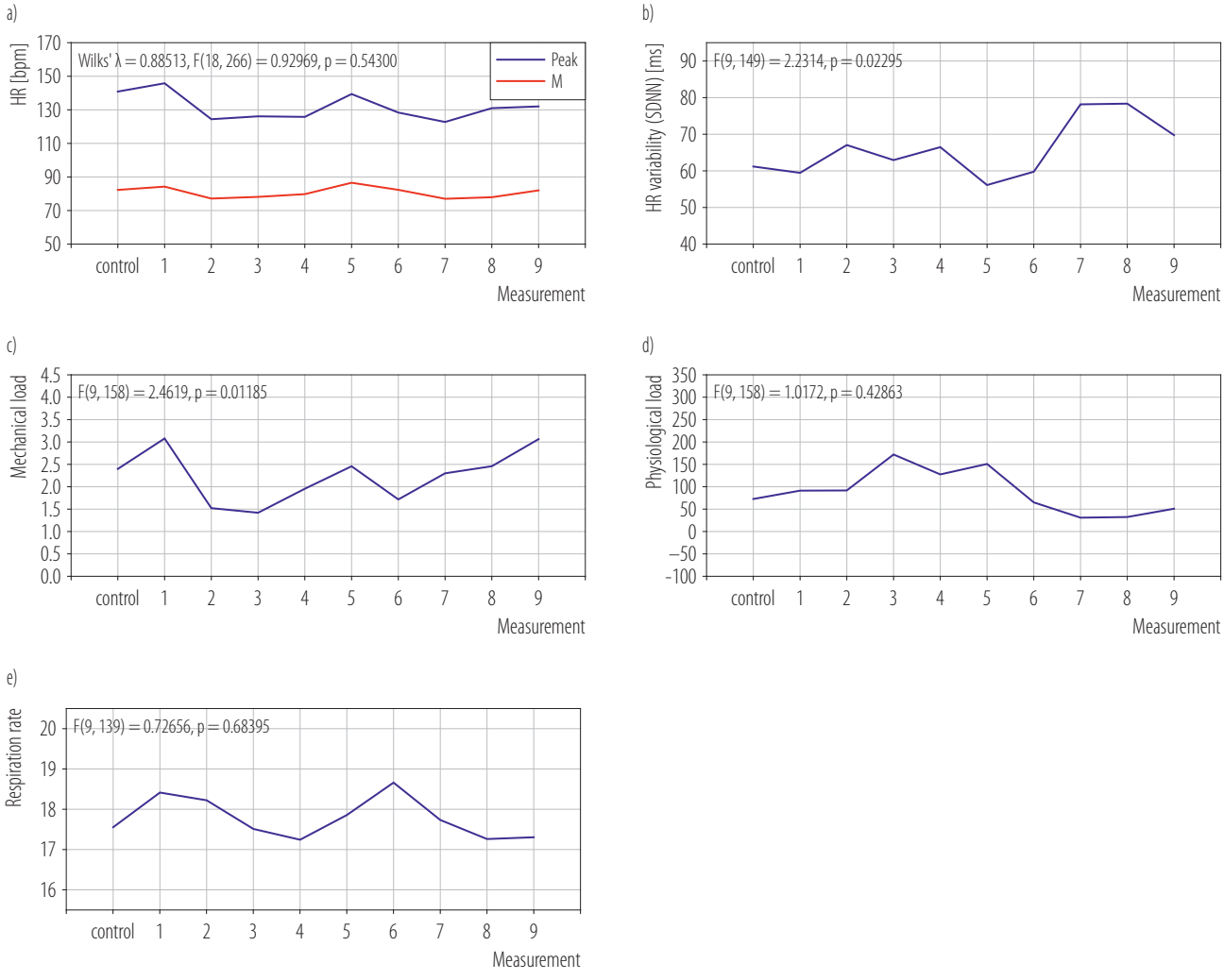


Figure 7. Performance metrics during progressive sleep deprivation in the Determination Test: a) omitted stimuli and incorrect reactions, b) total reactions, correct reactions, and stimuli presented during sessions, c) response time and test duration; and in the Visual Pursuit Test: d) time of correct and incorrect responses, e) completed tasks and correct answers, and f) total execution time across all sessions, in the study on sleepiness biomarkers among 18 healthy adults (9 women, 9 men), Warsaw, Poland, 2015

using PLR and VEP, and to compare them with hippus fatigue wave parameters in the PST. Age, sex, and iris pigmentation affect PLR parameters [20]. Previous clinical studies have shown that PLR and VEP parameters are sensitive to ocular [28–34], neurological [21–27], and autonomic [14,37] dysfunction. In the present study, this literature is not used to infer pathology, but to justify strict participant screening and cautious physiological interpretation. Because pupillary and VEP measures can be affected by ocular disease, afferent visual-pathway dysfunction [35,36], autonomic neuropathy, medication use, and neurological disorders, these factors were addressed

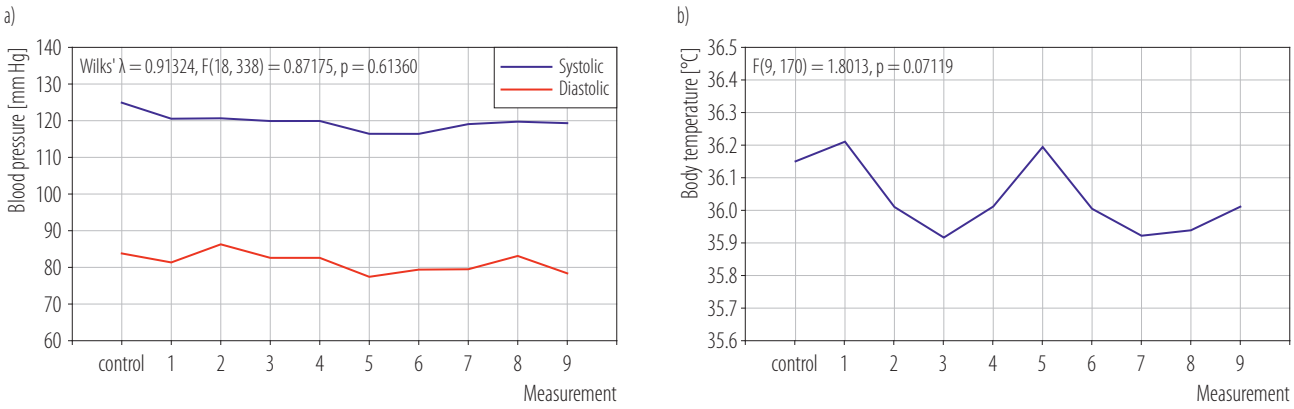


Peak and mean HR across all sessions showed daytime elevations during measurement 5 followed by nocturnal decline. Heart rate variability (SDNN) demonstrated significant increases during measurements 7–9, indicative of enhanced parasympathetic modulation during advanced fatigue. Mechanical load increased progressively with prolonged wakefulness. Physiological load showed corresponding decreases as autonomic resources were redistributed. Respiration rate decreased during nighttime measurements.

Figure 8. Physiological responses during 48 h of sustained wakefulness recorded with the Zephyr BioHarness 3 system: a) peak and mean heart rate (HR) across all sessions, b) HR variability (standard deviation of normal-to-normal intervals – SDNN), c) mechanical load, d) physiological load, and e) respiration rate, in the study on sleepiness biomarkers among 18 healthy adults (9 women, 9 men), Warsaw, Poland, 2015

through exclusion criteria, ophthalmological assessment, and medication/substance-use screening. Accordingly, the observed changes should be interpreted as state-dependent effects of sustained wakefulness in healthy adults rather than as markers of structural visual-pathway disease. This distinction is important because it supports the internal validity of the sleep-deprivation interpretation while limiting direct generalization to clinical populations.

Studies have explored PLR behavior during prolonged wakefulness, noting decreased pupil diameter during sleep deprivation without changes in reflex LAT or constriction amplitude due to limited sensor resolution [38]. Studies analyzing hourly PLR responses over 24 h using



Systolic and diastolic blood pressure showed modest reductions relative to baseline, with peak decreases of 7% during measurements 5–6. Core body temperature exhibited small but consistent declines during nighttime measurements (−0.24°C and −0.23°C).

Figure 9. Cardiovascular and thermoregulatory changes during sustained wakefulness: a) systolic and diastolic blood pressure, and b) core body temperature, in the study on sleepiness biomarkers among 18 healthy adults (9 women, 9 men), Warsaw, Poland, 2015

chromatic stimuli have revealed circadian modulation of redilation parameters under blue light stimulation (463 nm), corresponding to ipRGC activation [39]. Studies have found that RA and CV decrease with fatigue, correlating with sleepiness [40]. Research has reported prolonged pupillary LAT and half-reaction time following sleep deprivation and alcohol exposure [10], while their 2025 study showed increased pupil redilation velocity under acute sleep deprivation (M±SD 0.22 ± 0.03 mm/s vs. 0.20 ± 0.03 mm/s, p = 0.004) [41]. These findings align with the current results for the parameters V_{Dil1} and V_{Dil2} (Figure 2e,f), indicating redilation acceleration with increasing wakefulness. The experiment showed that 4 PLR-derived parameters – D_{Dil1}, D_{Dil2}, V_{Dil1}, and V_{Dil2} – changed with progressive sleep deprivation, suggesting potential fatigue biomarkers. While increases in RA with sleep loss align with previous findings [40,42], the D_{Dil1} and D_{Dil2} parameters provide a more sensitive reflection of the parasympathetic modulation. Physiologically, this reflects parasympathetic drive dominance during fatigue, facilitating faster constriction and altered redilation dynamics. Increases in V_{Dil1} and V_{Dil2} during the second night (Figure 2e,f) suggest compensatory sympathetic pathway activation, maintaining readiness despite mounting sleep pressure. These observations indicate that PLR dynamics, particularly D_{Dil1}, D_{Dil2}, V_{Dil1}, and V_{Dil2}, may serve as sensitive, non-invasive markers of neurophysiological fatigue, complementing classical indices like RA or LAT. Reaction duration showed only limited point-wise evidence and should therefore be interpreted as supportive rather than as a stable primary marker.

Parameters from PST, including the rPUI, BLK, and INT, increased across measurements [43,44]. The rPUI and INT elevations emerged after 24 h of wakefulness and persisted for 48 h, indicating fatigue. The correlation between PST and PLR highlights the shared autonomic substrates. The PST results mirrored SSS scores, with sleepiness increasing 150% before and 141% after PST at study end. These findings validate the PLR as a rapid PST analog, offering similar sensitivity in less time.

Further research is needed to clarify the contributions of the parasympathetic nervous system (PNS) and sympathetic nervous system (SNS) to hippus modulation. Studies have shown that PNS suppression reduces pupillary oscillations, whereas SNS activation expands the pupil without affecting the hippus waveform [16,45].

Table 8. Omnibus repeated-measures analysis of variance (ANOVA) with false discovery rate (FDR) correction in 18 healthy adults (9 women, 9 men), Warsaw, Poland, 2015

Parameter	Participants (N = 18) [n]	df		F	p	q FDR	Partial η^2	FDR sig.
		effect	error					
Pupillary light reflex								
latency [s]	16	9	135	2.56	0.010	0.014	0.15	yes
reaction duration [s]	16	9	135	1.28	0.254	0.254	0.08	no
time of minimum diameter [s]	16	9	135	2.51	0.011	0.015	0.14	yes
D_{Dil1} [mm]	16	9	135	6.11	<0.001	<0.001	0.29	yes
D_{Dil2} [mm]	16	9	135	7.33	<0.001	<0.001	0.33	yes
V_{Dil1} [mm/s]	16	9	135	3.26	0.001	0.003	0.18	yes
V_{Dil2} [mm/s]	16	9	135	5.57	<0.001	<0.001	0.27	yes
relative amplitude [%]	16	9	135	3.68	<0.001	0.001	0.20	yes
contraction velocity [mm/s]	16	9	135	1.29	0.249	0.254	0.08	no
redilation time [s]	16	9	135	2.74	0.006	0.010	0.15	yes
contraction time [s]	16	9	135	2.47	0.012	0.015	0.14	yes
initial pupil diameter [mm]	16	9	135	3.33	0.001	0.003	0.18	yes
PST/SSS								
$rPUI_{all}$	18	9	153	16.62	<0.001	<0.001	0.49	yes
SSS_{before}	18	9	153	35.40	<0.001	<0.001	0.68	yes
SSS_{after}	18	9	153	50.77	<0.001	<0.001	0.75	yes
$pupil_{ALL}$	18	9	153	4.35	<0.001	<0.001	0.20	yes
hippus wave interpolation	18	9	153	26.17	<0.001	<0.001	0.61	yes
blinks	18	9	153	4.91	<0.001	<0.001	0.22	yes
$rPUI_5$	18	9	153	15.20	<0.001	<0.001	0.47	yes
$rPUI_6$	18	9	153	13.69	<0.001	<0.001	0.45	yes
$rPUI_7$	18	9	153	13.69	<0.001	<0.001	0.45	yes
VEP pattern								
N75 [ms]	18	2	34	1.11	0.341	0.455	0.06	no
P100 [ms]	16	2	30	5.11	0.012	0.025	0.25	yes
N145 [ms]	18	2	34	11.45	<0.001	<0.001	0.40	yes
75–100 (μV)	18	2	34	0.07	0.928	0.928	0.00	no
DT								
response time (Me) [ms]	18	4	68	4.43	0.003	0.004	0.21	yes
correct reaction [n]	18	4	68	4.57	0.002	0.004	0.21	yes
incorrect reaction [n]	18	4	68	0.61	0.654	0.654	0.03	no
omitted stimuli [n]	18	4	68	4.57	0.002	0.004	0.21	yes

Table 8. Omnibus repeated-measures analysis of variance (ANOVA) with false discovery rate (FDR) correction in 18 healthy adults (9 women, 9 men), Warsaw, Poland, 2015 – cont.

Parameter	Participants (N = 18) [n]	df		F	p	q FDR	Partial η^2	FDR sig.
		effect	error					
LVT								
correct response time [s]	17	9	144	2.32	0.018	0.073	0.13	no
execution time [s]	17	9	144	1.82	0.069	0.138	0.10	no
correct reaction [n]	17	9	144	1.53	0.142	0.190	0.09	no
completed [n]	17	9	144	0.83	0.593	0.593	0.05	no

DT – Determination Test; LVT – Visual Pursuit Test (*Linienverfolgungstest*); PST – pupillary sleepiness test; SSS – *Stanford Sleepiness Scale*.
For description of N75, N145, and P100 see Table 2.
Dil1 – fast dilation phase; Dil2 – slow dilation phase; df – degrees of freedom; FDR sig. – significance after FDR correction; rPUI – relative pupillary unrest index; V_{Dil1} – fast redilation velocity; V_{Dil2} – slow redilation velocity; VEP – visual evoked potential.
All analyses were performed on participant-level data. False discovery rate correction used the Benjamini-Hochberg procedure within predefined outcome families; q values denote FDR-adjusted p values. Visual evoked potential analyses were restricted to pattern-VEP components available in the exported dataset (N75, P100, N145, and 75–100 amplitude).

This supports the hypothesis that hippus arises from central parasympathetic activity. Although rPUI shows inter-individual variability [46], absolute rPUI values of 1 mm/s occur after 1 night of sleep deprivation [40]. Visual evoked potential analysis confirmed cortical visual processing sensitivity to sleep deprivation. With increasing time awake, latency increased for N145 and P100 but remained stable for N75, suggesting that fatigue affects later stages of cortical visual processing more than the earliest stage. These results support previous findings of N145 LAT prolongation as a fatigue-related perceptual slowing correlate [47]. Significant LAT shifts occurred in most configurations, except 1 (>48 h, right eye, left-field stimulation) (Table 5). The absence of systematic interocular asymmetry supports the interpretation that the observed VEP LAT changes reflected state-dependent modulation during prolonged wakefulness rather than unilateral ocular or afferent pathway dysfunction. Future studies should extend VEP protocols to include flash VEP paradigms. Psychometric assessments showed that the participants maintained adequate cognitive performance. Fluctuations in the NASA-TLX effort score, particularly among evening chronotypes, may reflect compensatory recruitment of cortical resources [48]. Cardiovascular parameters and body temperature stability indicate the effects of neurocognitive fatigue. The findings show that pupillary and cortical electrophysiological indices are markers of sleep deprivation–induced fatigue. The PLR offers a rapid approach to assess autonomic balance. The coherence between the PLR, PST, and VEP measurements supports their combined use for monitoring alertness. Although sleep deprivation was standardized, psychological tests provided a general cognitive assessment. Future research should incorporate specialized cognitive batteries to capture the temporal fluctuations in cortical activation. The integration of PLR, PST, and VEP analyses demonstrated their potential as indicators of sleep-related fatigue.

Exploratory convergent-validity analyses suggested partially overlapping but non-identical physiological layers. This supports an exploratory interpretation and indicates that PLR, PST, and VEP may capture complementary rather than fully redundant aspects of progressive sleepiness.

Table 9. Key baseline-to-deprivation contrasts and paired effect sizes in 18 healthy adults (9 women, 9 men), Warsaw, Poland, 2015

Parameter	Contrast	Participants (N = 18) [n]	Baseline (M)	Session (M)	MD	95% CI	p	q FDR	Cohen d_z	FDR sig.
Pupillary light reflex (PLR)										
latency [s]	baseline vs. S9	18	0.283	0.293	0.010	0.001–0.019	0.025	0.028	0.58	yes
TMD [s]	baseline vs. S8	16	0.814	0.864	0.050	0.019–0.080	0.003	0.009	0.87	yes
TMD endpoint [s]	baseline vs. S9	18	0.810	0.839	0.029	–0.025–0.083	0.269	0.269	0.27	no
D_{Dil1} [mm]	baseline vs. S9	18	3.736	2.705	–1.030	–1.546–(–0.515)	<0.001	0.002	–0.99	yes
D_{Dil2} [mm]	baseline vs. S9	18	5.307	4.037	–1.269	–1.864–(–0.675)	<0.001	0.002	–1.06	yes
V_{Dil1} [mm/s]	baseline vs. S9	18	1.830	2.603	0.773	0.215–1.332	0.010	0.015	0.69	yes
V_{Dil2} [mm/s]	baseline vs. S9	18	0.580	1.497	0.917	0.322–1.511	0.005	0.009	0.77	yes
relative amplitude [%]	baseline vs. S9	18	20.227	22.862	2.634	0.445–4.824	0.021	0.028	0.60	yes
PST [mm/s]										
$rPUI_{all\ first\ robust}$	baseline vs. S4	18	0.788	1.312	0.523	0.310–0.736	<0.001	<0.001	1.22	yes
$rPUI_{all\ endpoint}$	baseline vs. S9	18	0.788	1.558	0.769	0.465–1.074	<0.001	<0.001	1.26	yes
VEP [ms]										
P100	baseline vs. 48 h	16	110.729	115.760	5.031	0.928–9.135	0.020	0.020	0.65	yes
N145	baseline vs. 48 h	18	156.204	170.935	14.731	6.644–22.819	0.001	0.003	0.91	yes
SSS [pts]										
SSS_{before}	baseline vs. S9	18	2.000	5.000	3.000	2.385–3.615	<0.001	<0.001	2.43	yes
DT [ms]										
response time (Me)	baseline vs. 48 h	18	702.222	692.222	–10.000	–39.983–19.983	0.491	0.491	–0.17	no
LVT [s]										
correct response time	baseline vs. S9	18	2.950	3.080	0.130	–0.199–0.459	0.416	0.416	0.20	no

S4, S8 and S9 – measurement 4, 8 and 9; 48 h – measurement at 48 h; MD – mean difference; TMD – time of minimum diameter.
Other abbreviations as in Table 8.
All analyses were performed on participant-level data. False discovery rate correction used the Benjamini-Hochberg procedure within predefined outcome families; q values denote FDR-adjusted p values. Cohen's d_z was calculated for paired within-subject contrasts as mean change divided by the SD of the change score. Visual evoked potential analyses were restricted to pattern-VEP components available in the exported dataset (N75, P100, N145, and 75–100 amplitude).

Table 10. Exploratory convergent-validity correlations in 18 healthy adults (9 women, 9 men), Warsaw, Poland, 2015

Variable pair	Participants (N = 18) [n]	Pearson r	p	q FDR	Spearman ρ	p	q FDR
ΔrPUI_all_9 vs. ΔSSS_before_9	18	0.33	0.181	0.571	0.30	0.223	0.916
ΔrPUI_all_9 vs. ΔSSS_after_9	18	0.36	0.142	0.544	0.31	0.205	0.916
ΔLat_9 vs. ΔSSS_before_9	18	0.07	0.787	0.973	–0.06	0.817	0.987
ΔTMD_9 vs. ΔSSS_before_9	18	–0.13	0.605	0.973	–0.11	0.665	0.987
ΔD_{Dil1}_9 vs. ΔSSS_before_9	18	–0.25	0.315	0.725	–0.17	0.500	0.987
ΔD_{Dil2}_9 vs. ΔSSS_before_9	18	–0.47	0.046	0.388	–0.40	0.096	0.916
ΔLat_9 vs. ΔrPUI_all_9	18	–0.16	0.524	0.973	–0.02	0.922	0.987
ΔTMD_9 vs. ΔrPUI_all_9	18	–0.10	0.680	0.973	–0.16	0.532	0.987
ΔD_{Dil1}_9 vs. ΔrPUI_all_9	18	–0.56	0.015	0.339	–0.43	0.073	0.916
ΔD_{Dil2}_9 vs. ΔrPUI_all_9	18	–0.43	0.072	0.388	–0.26	0.307	0.916
ΔV_{Dil1}_9 vs. ΔrPUI_all_9	18	0.28	0.268	0.686	0.22	0.376	0.960
ΔV_{Dil2}_9 vs. ΔrPUI_all_9	18	0.17	0.491	0.973	–0.02	0.929	0.987
ΔN145_48h vs. ΔrPUI_all_9	18	0.46	0.053	0.388	0.27	0.287	0.916
ΔP100_48h vs. ΔrPUI_all_9	16	0.02	0.931	0.973	–0.11	0.678	0.987
ΔN145_48h vs. ΔSSS_before_9	18	0.32	0.199	0.571	0.30	0.224	0.916
ΔP100_48h vs. ΔSSS_before_9	16	–0.14	0.605	0.973	–0.27	0.319	0.916
ΔrPUI_all_9 vs. ΔDT_RT_ms_48h	18	–0.03	0.916	0.973	–0.02	0.951	0.987
ΔrPUI_all_9 vs. ΔDT_correct_48h	18	0.05	0.842	0.973	0.00	0.987	0.987
ΔrPUI_all_9 vs. ΔDT_omitted_48h	18	–0.10	0.698	0.973	–0.11	0.666	0.987
ΔrPUI_all_9 vs. ΔLVT_correct_time_s_9	18	0.04	0.879	0.973	–0.01	0.981	0.987
ΔrPUI_all_9 vs. ΔLVT_execution_s_9	18	0.09	0.732	0.973	0.05	0.842	0.987
ΔN145_48h vs. ΔDT_RT_ms_48h	18	–0.00	0.988	0.988	0.08	0.744	0.987
ΔN145_48h vs. ΔLVT_correct_time_s_9	18	0.42	0.084	0.388	0.09	0.723	0.987

delta – baseline-normalized change; Lat – latency; _9 – at measurement 9; _48h – at the 48-h measurement.
Other abbreviations and explanations as in Tables 8 and 9.

Table 11. Exploratory sex-stratified endpoint-change comparisons in 18 healthy adults (9 women, 9 men), Warsaw, Poland, 2015

Parameter	Contrast	Women			Men			p[a]	q FDR
		baseline (M±SD)	endpoint (M±SD)	change (M±SD)	baseline (M±SD)	endpoint (M±SD)	change (M±SD)		
Latency [ms]	baseline vs. S9	281.1±17.9	295.6±19.8	14.5±19.4	285.1±19.9	291.2±19.6	6.1±15.8	0.326	0.802
Time of minimum diameter [s]	baseline vs. S9	0.808±0.052	0.848±0.118	0.041±0.138	0.813±0.051	0.831±0.089	0.017±0.073	0.656	0.875
D_{Dil1} [mm]	baseline vs. S9	3.53±0.94	2.29±0.93	−1.24±0.86	3.94±1.04	3.12±0.92	−0.82±1.20	0.401	0.802
D_{Dil2} [mm]	baseline vs. S9	5.08±0.94	3.73±1.19	−1.35±0.84	5.53±1.02	4.34±1.06	−1.19±1.52	0.787	0.875
rPUI [s^{-1}]	baseline vs. S9	0.73±0.37	1.68±0.24	0.95±0.33	0.85±0.55	1.44±0.57	0.59±0.78	0.229	0.802
SSS before test score	baseline vs. S9	2.00±0.50	5.11±0.93	3.11±0.78	2.00±1.00	4.89±1.36	2.89±1.62	0.717	0.875
N145 latency [ms]	baseline vs. 48 h	154.9±16.6	169.9±22.9	14.9±15.2	157.5±15.6	172.0±15.9	14.5±18.2	0.958	0.958
P100 latency [ms]	baseline vs. 48 h	110.5±7.0	112.5±5.4	1.9±4.9	110.9±6.0	118.3±9.3	7.4±8.8	0.138	0.802
DT reaction time [ms]	baseline vs. 48 h	721.1±63.1	716.7±100.4	−4.4±57.0	683.3±67.3	667.8±93.1	−15.6±66.4	0.708	0.875
LVT correct-response time [s]	baseline vs. S9	2.97±0.26	2.92±0.35	−0.05±0.39	2.93±0.47	3.24±0.98	0.31±0.84	0.258	0.802

Abbreviations as in Tables 8 and 9.

All analyses were performed on participant-level data. Visual evoked potential (VEP) analyses were restricted to pattern-VEP components available in the exported dataset (N75, P100, N145, and 75–100 amplitude). Women: N = 9 for all listed comparisons except P100 latency, where N = 7 because of valid paired VEP recordings. Men: N = 9. Sex differences were tested on endpoint change scores. P values are nominal p values for exploratory sex-difference comparisons; q FDR values are Benjamini-Hochberg-adjusted values within the sex-stratified exploratory comparison family. No sex-dependent endpoint-change comparison remained significant after FDR correction. Latency values are presented in milliseconds for readability.

[a] For sex difference in change.

Several limitations should be considered. The sample size was constrained by the demanding 48-hour supervised sleep-deprivation protocol. Sensitivity analysis indicated that the study could detect moderate-to-large within-subject effects, whereas small effects and subgroup differences, particularly in secondary behavioral or cardiovascular outcomes, may have remained undetected. Although sex-stratified exploratory analyses were added, the subgroup size was small; therefore, the study was not powered to draw definitive conclusions about sex-related differences in pupillometric or VEP responses to sleep deprivation. Exploratory convergent-validity correlations did not remain significant after FDR correction across the full correlation family; therefore, cross-modal associations should be interpreted as hypothesis-generating.

These findings support the further development of non-invasive visual biomarkers for sleepiness assessment in clinical, ergonomic, and safety-critical contexts. However, the present results should be interpreted as evidence for candidate biomarkers under controlled laboratory conditions rather than as direct validation of an operational diagnostic tool. Further studies should verify classification performance, test-retest reliability, and field applicability in occupational groups exposed to acute and chronic sleep loss.

CONCLUSIONS

This study showed that prolonged wakefulness produces a structured visual physiological profile of progressive sleepiness in healthy adults. The most robust pupillometric findings involved PLR LAT, TMD, and dilation-phase recovery parameters, particularly D_{Dil1}, D_{Dil2}, V_{Dil1}, and V_{Dil2}. The PST-derived rPUI provided the principal tonic marker of pupillary instability, whereas pattern-VEP P100 and N145 latencies added a cortical visual-response component. Brief psychophysiological tasks showed non-monotonic, task-dependent changes and did not provide a deterioration pattern comparable to the pupillometric and VEP markers. The findings support PLR, PST/rPUI, and pattern-VEP measures as complementary candidate biomarkers of progressive sleepiness under controlled total sleep-deprivation conditions. Their clinical, ergonomic, and occupational use requires further validation in larger and field-based cohorts.

AUTHOR CONTRIBUTIONS

Research concept: Krzysztof Różanowski
Research methodology: Krzysztof Różanowski, Michał Jankowski
Collecting material: Krzysztof Różanowski
Statistical analysis: Krzysztof Różanowski
Interpretation of results: Krzysztof Różanowski, Michał Jankowski
References: Krzysztof Różanowski, Michał Jankowski

REFERENCES

1. Kim D-J, Lee H-P, Kim MS, Park Y-J, Go H-J, Kim K-S, et al. The effect of total sleep deprivation on cognitive functions in normal adult male subjects. Int J Neurosci. 2001;109(1-2): 127-37. https://doi.org/10.3109/00207450108986529.
2. Schnyer DM, Zeithamova D, Williams V. Decision-making under conditions of sleep deprivation: cognitive and neural consequences. Mil Psychol. 2009;21(Suppl 1):S36-45. https://doi.org/10.1080/08995600802554607.
3. Klumpers UMH, Veltman DJ, Van Tol M-J, Kloet RW, Boellaard R, Lammertsma AA, et al. Neurophysiological effects of sleep deprivation in healthy adults, a pilot study. PLoS One. 2015;10(1):e0116906. https://doi.org/10.1371/journal.pone.0116906.
4. Goel N, Rao H, Durmer JS, Dinges DF. Neurocognitive consequences of sleep deprivation. Semin Neurol. 2009;29(4): 320-39. https://doi.org/10.1055/s-0029-1237117.
5. Dinges DF, Pack F, Williams K, Gillen KA, Powell JW, Ott GE, et al. Cumulative sleepiness, mood disturbance, and psycho-

motor vigilance performance decrements during a week of sleep restricted to 4–5 hours per night. Sleep. 1997;20(4): 267-77. https://doi.org/10.1093/sleep/20.4.267.

6. Cazzoli D, Antoniades CA, Kennard C, Nyffeler T, Bassetti CL, Müri RM. Eye movements discriminate fatigue due to chronotypical factors and time spent on task – a double dissociation. PLoS One. 2014;9(1):e87146. https://doi.org/10.1371/journal.pone.0087146.
7. Odle-Dusseau HN, Bradley JL, Pilcher JJ. Subjective perceptions of the effects of sustained performance under sleep-deprivation conditions. Chronobiol Int. 2010;27(2):318-33. https://doi.org/10.3109/07420520903502226.
8. Lowrie J, Brownlow H. The impact of sleep deprivation and alcohol on driving: a comparative study. BMC Public Health. 2020;20(1):980. https://doi.org/10.1186/s12889-020-09095-5.
9. Kaida K, Niki K. Total sleep deprivation decreases flow experience and mood status. Neuropsychiatr Dis Treat. 2014; 10:19-25. https://doi.org/10.2147/NDT.S53633.
10. Kaifie A, Reugels M, Kraus T, Kursawe M. The pupillary light reflex (PLR) as a marker for the ability to work or drive – a feasibility study. J Occup Med Toxicol. 2021;16:39. https://doi.org/10.1186/s12995-021-00330-2.
11. Phurailatpam J. Evoked potentials: visual evoked potentials (VEPs): clinical uses, origin, and confounding parameters. J Med Soc. 2014;28(3):140-44. https://doi.org/10.4103/0972-4958.148494.
12. Emerson RG, Pedley TA. Chapter 32A – Clinical neurophysiology: electroencephalography and evoked potentials. In: Bradley's Neurology in Clinical Practice. Elsevier; 2012. p. 368-93. https://doi.org/10.1016/B978-1-4377-0434-1.00032-3.
13. Šuštar Habjan M, Bach M, Van Genderen MM, Li S, Mizota A, Nilsson J, et al. ISCEV standard for clinical visual evoked potentials (2025 update). Doc Ophthalmol. 2025;151(2):97-112. https://doi.org/10.1007/s10633-025-10042-1.
14. Hall CA, Chilcott RP. Eyeing up the future of the pupillary light reflex in neurodiagnostics. Diagnostics (Basel). 2018;8(1):19. https://doi.org/10.3390/diagnostics8010019.
15. Joshi S, Li Y, Kalwani RM, Gold JI. Relationships between pupil diameter and neuronal activity in the locus coeruleus, colliculi, and cingulate cortex. Neuron. 2016;89(1):221-34. https://doi.org/10.1016/j.neuron.2015.11.028.
16. Turnbull PRK, Irani N, Lim N, Phillips JR. Origins of pupillary hippus in the autonomic nervous system. Invest Ophthalmol Vis Sci. 2017;58(1):197-203. https://doi.org/10.1167/iovs.16-20785.
17. Benditt DG, Fedorowski A, Sutton R, Van Dijk JG. Pathophysiology of syncope: current concepts and their development. Physiol Rev. 2025;105(1):209-66. https://doi.org/10.1152/physrev.00007.2024.
18. Vrettou CS, Fragkou PC, Mallios I, Barba C, Giannopoulos C, Gavrielatou E, et al. The role of automated infrared pupillometry in traumatic brain injury: a narrative review. J Clin Med. 2024;13(2):614. https://doi.org/10.3390/jcm13020614.
19. Zele AJ, Gamlin PD, editors. The Pupil: Behavior, Anatomy, Physiology and Clinical Biomarkers. Frontiers Media SA; 2020. https://doi.org/10.3389/978-2-88963-756-0.
20. Sharma S, Baskaran M, Rukmini AV, Nongpiur ME, Htoon H, Cheng C-Y, et al. Factors influencing the pupillary light reflex in healthy individuals. Graefes Arch Clin Exp Ophthalmol. 2016; 254(7):1353-9. https://doi.org/10.1007/s00417-016-3311-4.
21. De Rodez Benavent SA, Nygaard GO, Harbo HF, Tønnesen S, Sowa P, Landrø NI, et al. Fatigue and cognition: pupillary responses to problem-solving in early multiple sclerosis patients. Brain Behav. 2017;7(7):e00717. https://doi.org/10.1002/brb3.717.
22. Van Stavern GP, Bei L, Shui Y-B, Huecker J, Gordon M. Pupillary light reaction in preclinical Alzheimer's disease subjects compared with normal ageing controls. Br J Ophthalmol. 2018;103(7):971-5. https://doi.org/10.1136/bjophthalmol-2018-312425.
23. Chougule PS, Najjar RP, Finkelstein MT, Kandiah N, Milea D. Light-induced pupillary responses in Alzheimer's disease. Front Neurol. 2019;10:360. https://doi.org/10.3389/fneur.2019.00360.
24. Romagnoli M, Stanzani Maserati M, De Matteis M, Capellari S, Carbonelli M, Amore G, et al. Chromatic pupillometry

findings in Alzheimer's disease. Front Neurosci. 2020;14: 780. https://doi.org/10.3389/fnins.2020.00780.

25. Feigl B, Dumpala S, Kerr GK, Zele AJ. Melanopsin cell dysfunction is involved in sleep disruption in Parkinson's disease. J Parkinsons Dis. 2020;10(4):1467-1476. https://doi.org/10.3233/JPD-202178.
26. Giza E, Fotiou D, Bostantjopoulou S, Katsarou Z, Karlovasitou A. Pupil light reflex in Parkinson's disease: evaluation with pupillometry. Int J Neurosci. 2011;121(1):37-43. https://doi.org/10.3109/00207454.2010.526730.
27. Gaynes BI, Zaffer A, Yousefzai R, Chazaro-Cortes M, Colletta K, Kletzel SL, et al. Variable abnormality of the melanopsin-derived portion of the pupillary light reflex (PLR) in patients with Parkinson's disease (PD) and parkinsonism features. Neurol Sci. 2022;43(1):349-56. https://doi.org/10.1007/s10072-021-05245-8.
28. Moura ALA, Nagy BV, La Morgia C, Barboni P, Oliveira AGF, Salomão SR, et al. The pupil light reflex in Leber's hereditary optic neuropathy: evidence for preservation of melanopsin-expressing retinal ganglion cells. Invest Ophthalmol Vis Sci. 2013;54(7):4471-7. https://doi.org/10.1167/iovs.12-11137.
29. Gracitelli CPB, Duque-Chica GL, Moura AL, Nagy BV, De Melo GR, Roizenblatt M, et al. A positive association between intrinsically photosensitive retinal ganglion cells and retinal nerve fiber layer thinning in glaucoma. Invest Ophthalmol Vis Sci. 2014;55(12):7997-8005. https://doi.org/10.1167/iovs.14-15146.
30. Duque-Chica GL, Gracitelli CPB, Moura ALA, Nagy BV, Vidal KS, Paranhos A Jr, et al. Inner and outer retinal contributions to pupillary light response: correlation to functional and morphologic parameters in glaucoma. J Glaucoma. 2018;27(8):723-32. https://doi.org/10.1097/IJG.0000000000001003.
31. Feigl B, Zele AJ. Melanopsin-expressing intrinsically photosensitive retinal ganglion cells in retinal disease. Optom Vis Sci. 2014;91(8):894-903. https://doi.org/10.1097/OPX.0000000000000284
32. Duque-Chica GL, Gracitelli CPB, Moura ALA, Nagy BV, Vidal KS, De Melo G, et al. Contributions of the melanopsin-expressing ganglion cells, cones, and rods to the pupillary light response in obstructive sleep apnea. Invest Ophthalmol Vis Sci. 2019;60(8):3002-12. https://doi.org/10.1167/iovs.19-26944.
33. Park JC, Moura AL, Raza AS, Rhee DW, Kardon RH, Hood DC. Toward a clinical protocol for assessing rod, cone, and melanopsin contributions to the human pupil response. Invest Ophthalmol Vis Sci. 2011;52(9):6624-35. https://doi.org/10.1167/iovs.11-7586.
34. Feigl B, Mattes D, Thomas R, Zele AJ. Intrinsically photosensitive (melanopsin) retinal ganglion cell function in glaucoma. Invest Ophthalmol Vis Sci. 2011;52(7):4362-7. https://doi.org/10.1167/iovs.10-7069.
35. Gooley JJ, Ho Mien I, St Hilaire MA, Yeo S-C, Chua EC-P, Van Reen E, et al. Melanopsin and rod-cone photoreceptors play different roles in mediating pupillary light responses during exposure to continuous light in humans. J Neurosci. 2012;32(41):14242-53. https://doi.org/10.1523/JNEUROSCI.1321-12.2012.
36. Kostic C, Crippa SV, Martin C, Kardon RH, Biel M, Arsenijevic Y, et al. Determination of rod and cone influence to the early and late dynamic of the pupillary light response. Invest Ophthalmol Vis Sci. 2016;57(6):2501-8. https://doi.org/10.1167/iovs.16-19150.
37. Kvamme TL, Pedersen MU, Overgaard M, Rømer Thomsen K, Voon V. Pupillary reactivity to alcohol cues as a predictive biomarker of alcohol relapse following treatment in a pilot study. Psychopharmacology (Berl). 2019;236(4): 1233-43. https://doi.org/10.1007/s00213-018-5131-1.
38. Ranzijn R, Lack L. The pupillary light reflex cannot be used to measure sleepiness. Psychophysiology. 1997;34(1):17-22. https://doi.org/10.1111/j.1469-8986.1997.tb02411.x.
39. Münch M, Léon L, Crippa SV, Kawasaki A. Circadian and wake-dependent effects on the pupil light reflex in response to narrow-bandwidth light pulses. Invest Ophthalmol Vis Sci. 2012;53(8):4546-55. https://doi.org/10.1167/iovs.12-9494.

40. Różanowski K, Bernat M, Kamińska A. Estimation of operators' fatigue using optical methods for determination of pupil activity. Int J Occup Med Environ Health. 2015;28(2): 263-81. https://doi.org/10.13075/ijomeh.1896.00274.
41. Ozkoyuncu Kocabas D, Atalay B, Taskiran Sag A. Static and dynamic pupillary changes reflect autonomic effects of acute sleep deprivation in healthy adults. Sleep Med. 2025; 136:106795. https://doi.org/10.1016/j.sleep.2025.106795.
42. Różanowski K. New biomarkers for the assessment of fatigue evoked by long-term sleep deprivation based on pupillary light reflex using rheological models. Biocybern Biomed Eng. 2022;42(4):1162-82. https://doi.org/10.1016/j.bbe.2022.09.006.
43. Różanowski K, Lewandowski J, Murawski K. Multifunctional, optical sensor for analysis of dynamic pupillary light reflex. Acta Phys Pol A. 2015;127(3):723-9. https://doi.org/10.12693/aphyspola.127.723.
44. Warga M, Lüdtke H, Wilhelm H, Wilhelm B. How do spontaneous pupillary oscillations in light relate to light intensity? Vision Res. 2009;49(3):295-300. https://doi.org/10.1016/j.visres.2008.09.019.
45. Piu P, Serchi V, Rosini F, Rufa A. A cross-recurrence analysis of the pupil size fluctuations in steady scotopic conditions. Front Neurosci. 2019;13:407. https://doi.org/10.3389/fnins.2019.00407.
46. Eggert T, Sauter C, Dorn H, Peter A, Hansen M-L, Danker-Hopfe H. Inter- and intraindividual variability of the pupillary unrest index. Somnologie (Berl). 2017;21(3):187-92. https://doi.org/10.1007/s11818-017-0128-2.
47. Rola R, Kozica A, Rozanowski K. P53-S The effect of sleep deprivation on the parameters of visual evoked potentials in healthy volunteers. Clin Neurophysiol. 2019;130(7):e110. https://doi.org/10.1016/j.clinph.2019.04.589.
48. Littner MR, Kushida C, Wise M, Davila DG, Morgenthaler T, Lee-Chiong T, et al. Practice parameters for clinical use of the multiple sleep latency test and the maintenance of wakefulness test. Sleep. 2005;28(1):113-21. https://doi.org/10.1093/sleep/28.1.113.

This work is available in Open Access model and licensed under a Creative Commons Attribution 4.0 International license – https://creativecommons.org/licenses/by/4.0/.